OPEN

Citation: Transl Psychiatry (2016) **6**, e943; doi:10.1038/tp.2016.211

www.nature.com/tp

ORIGINAL ARTICLE

Ankyrin-3 as a molecular marker of early-life stress and vulnerability to psychiatric disorders

A Luoni[1], R Massart[2], V Nieratschker[3,4], Z Nemoda[2,5], G Blasi[6], M Gilles[7], SH Witt[3], MJ Suderman[2,5,8], SJ Suomi[9], A Porcelli[6], G Rizzo[6], L Fazio[6], S Torretta[6], A Rampino[6], A Berry[10], P Gass[7], F Cirulli[10], M Rietschel[3], A Bertolino[6], M Deuschle[7], M Szyf[2,5] and MA Riva[1]

Exposure to early-life stress (ELS) may heighten the risk for psychopathology at adulthood. Here, in order to identify common genes that may keep the memory of ELS through changes in their methylation status, we intersected methylome analyses performed in different tissues and time points in rats, non-human primates and humans, all characterized by ELS. We identified *Ankyrin-3* (*Ank3*), a scaffolding protein with a strong genetic association for psychiatric disorders, as a gene persistently affected by stress exposure. In rats, *Ank3* methylation and mRNA changes displayed a specific temporal profile during the postnatal development. Moreover, exposure to prenatal stress altered the interaction of ankyrin-G, the protein encoded by *Ank3* enriched in the post-synaptic compartment, with PSD95. Notably, to model in humans a gene by early stress interplay on brain phenotypes during cognitive performance, we demonstrated an interaction between functional variation in *Ank3* gene and obstetric complications on working memory in healthy adult subjects. Our data suggest that alterations of *Ank3* expression and function may contribute to the effects of ELS on the development of psychiatric disorders.

Translational Psychiatry (2016) **6,** e943; doi:10.1038/tp.2016.211; published online 8 November 2016

INTRODUCTION

Adverse events during prenatal and early postnatal periods have a pivotal role in the later susceptibility to neuropsychiatric disorders[1–3] by interfering with the developmental trajectories of different systems, thus leading to long-lasting reprogramming consequences.[4] A growing body of evidence in the last decade has ascribed a key role to the epigenome, an array of chemical modifications to the DNA and histone proteins that affect gene expression without altering the DNA sequence, in bridging the experience of early insults with the appearance of a pathological phenotype at adulthood.[5–7] In particular, several rodent and human studies have proven that among epigenetic mechanisms, DNA methylation is dynamically sensitive to external cues particularly in the perinatal period, when most of the DNA methylation patterns are arranged to shape and define the cellular destiny and thus are also highly responsive and susceptible to environmental stressors that could alter such programming, thus increasing the vulnerability to later psychopathology.[8–13] In order to investigate the underlying causative mechanisms responsible of the long-term effects, several animal models have been developed that replicate the exposure to different types of stressors, of diverse intensities, in specific time windows during early perinatal life.[14–17] Although these animal models bear the advantages of studying, in few months, the effects of neonatal stress on adult behavior, both in the brain as well as at peripheral level, they have the limitation of lacking a direct relevance to the human condition. Here, in order to circumvent these problems, we used a cross-species genome-wide approach to identify shared DNA methylation patterns that are associated with early-life stress (ELS). In detail, we analyzed: (1) in humans the methylome signature characterizing $CD34^+$ cells derived from the cord blood of newborns whose mothers have been characterized for stressful experiences during the last trimester of gestation;[18] (2) in rhesus monkeys (*Macaca mulatta*) the DNA methylation patterns in the peripheral blood and in the prefrontal cortex (PFC) of monkeys that were exposed to different early-life social and rearing conditions;[19,20] (3) in rodents (*Rattus norvegicus*) we addressed the PFC of early-adult rats exposed to prenatal stress (PNS), a well-established model of vulnerability to altered adult behavior.[18,21–24]

This combined analysis pointed to *Ankyrin-3* (*Ank3*), a genetic risk factor for bipolar disorder and schizophrenia [25–27] that plays a pivotal role as scaffolding protein in specific membrane domains, such as the node of Ranvier and the axon initial segment.[28–30] Moreover, a role for ankyrin-G (ANKG) protein in regulating the post-synaptic compartment organization and function has recently emerged,[31,32] suggesting its potential for mediating the effects of stress exposure on dysfunctions associated with several psychiatric conditions.[33–36]

Finally, we demonstrated, in healthy adult subjects, that variation in the *Ank3* gene affecting gene expression interacted with an early stress factor (obstetric complications), in modulating prefrontostriatal connectivity and behavioral correlates of working memory, a cognitive phenotype tightly linked with different psychiatric disorders.[37] Overall, our results suggest that alterations

[1]Department of Pharmacological and Biomolecular Sciences, University of Milan, Milan, Italy; [2]Department of Pharmacology and Therapeutics, McGill University, Montreal, QC, Canada; [3]Department of Genetic Epidemiology in Psychiatry, Central Institute of Mental Health, Medical Faculty Mannheim/Heidelberg University, Mannheim, Germany; [4]Department of Psychiatry and Psychotherapy, University of Tuebingen, Tuebingen, Germany; [5]Sackler Institute for Epigenetics and Psychobiology, McGill University, Montreal, QC, Canada; [6]Department of Basic Medical Science, Neuroscience and Sense Organs, University of Bari Aldo Moro, Bari, Italy; [7]Department of Psychiatry and Psychotherapy, Central Institute of Mental Health, Medical Faculty Mannheim/Heidelberg University, Mannheim, Germany; [8]McGill Centre for Bioinformatics, McGill University, Montreal, QC, Canada; [9]Laboratory of Comparative Ethology, Eunice Kennedy Shriver National Institute of Child Health and Human Development, National Institutes of Health, Bethesda, MD, USA and [10]Department of Cell Biology and Neurosciences, Istituto Superiore di Sanità, Rome, Italy. Correspondence: Professor MA Riva, Department of Pharmacological and Biomolecular Sciences, University of Milan, Via Balzaretti 9, 20133 Milan, Italy.
E-mail: M.Riva@unimi.it
Received 1 April 2016; revised 11 July 2016; accepted 12 September 2016

of *Ank3* expression may contribute to the effects of perinatal stress on the vulnerability to psychiatric conditions.

MATERIALS AND METHODS

Human cohort for MeDIP-chip analysis

Data were obtained from a cohort of mothers and their infants ($n = 180$) recruited during the third trimester of pregnancy in the Rhine-Neckar Region of Germany. For inclusion and exclusion criteria see Supplementary Information. The study protocol was approved by the Ethics Committee of the Medical Faculty Mannheim of the University of Heidelberg. The study was conducted in accordance with the Declaration of Helsinki. All mothers provided written informed consent before participation. Investigator was blinded for the laboratory analyses.

Animals and experimental paradigms

Rhesus monkeys were reared as previously described.[18,19] Venous blood samples were obtained from 30 days old and 2-year-old monkeys, whole blood and buccal epithelial cell samples were taken at 2-years or older age, while PFCs were obtained from 7-year-old male monkeys. The Institutional Animal Care and Use Committee of the NICHD approved protocols for the use of experimental animals.

Pregnant rats were randomly assigned to control (Ctrl, $n = 7$) or PNS ($n = 9$) conditions. The stress paradigm was carried out as previously described.[18,38,39] Male offspring PFC was dissected at different postnatal days (PND: 7 (Ctrl, $n = 7$; PNS, $n = 9$), 21 (Ctrl, $n = 6$; PNS, $n = 6$) and 62 (Ctrl, $n = 7$; PNS, $n = 9$)). Rat handling and experimental procedures were performed in accordance with the EC guidelines (EC Council Directive 86/609 1987) and with the Italian legislation on animal experimentation (D. L. 116/92), in accordance with the National Institute of Health Guide for the Care and Use of Laboratory Animals.

All efforts were made to minimize animal suffering and to reduce the number of animals used, which has been set, using G*Power 3 software,[40] to take into account mortality and to allow $n = 7$–9 in each final group, also based upon our own previous data.[39] No pre-established inclusion/exclusion criteria were used for subsequent analyses. All samples were processed and analyzed by experimenters blind to rearing or prenatal stress conditions.

Extraction of DNA

Genomic DNA was extracted using Qiagen (Hilden, Germany) or Promega (Madison, WI, USA) systems, sheared by sonication and quantified using the Qubit system (Life Technologies, Burlington, ON, Canada).

Analysis of genome-wide promoter DNA methylation

MeDIP analysis was adapted from previously published protocols.[18,19] In detail, the final sample size for the methylome analysis was the following: rat PFC, Ctrl $N = 4$, PNS $N = 4$; human cohort, Ctrl $N = 8$, ELS $N = 10$; monkey PFC, Ctrl $N = 4$, ELS $N = 4$; monkey whole blood, Ctrl $N = 5$, ELS $N = 5$; monkey buccal samples, Ctrl $N = 3$, ELS $N = 3$; monkey $CD3^+$ (30 days old), Ctrl $N = 10$, ELS $N = 10$; monkey $CD3^+$ (2 years old), Ctrl $N = 6$, ELS $N = 4$ (the monkey $CD3^+$ samples were pooled and subjected to 3 parallel MeDIP analyses, that is 3 Ctrl and 3 ELS pools per time point). Briefly, 2 μg of DNA were sonicated, and methylated DNA was immunoprecipitated using anti-5-methyl-cytosine (Cat. No. BI-MECY-0100, Eurogentec, Fremont, CA, USA). The DNA–antibody complex was immunoprecipitated with protein G, and the methylated DNA was re-suspended in digestion buffer (50 mM TrisHCl pH8; 10 mM EDTA; 0.5 % SDS) and treated with proteinase K overnight at 55 °C. The input and bound fractions were purified, amplified using the Whole Genome Amplification Kit (Sigma-Aldrich, St. Louis, MO, USA), and labeled for microarray hybridization with Cy3-dUTP and Cy5-dUTP, respectively, using the CGH Enzymatic Labeling Kit (Agilent Technologies, Mississauga, ON, Canada) in accordance with the manufacturer's instructions. Custom designed tiling arrays were used (Agilent Technologies). All steps of the hybridization, washing, scanning and feature extraction procedures were performed in accordance with the Agilent Technologies protocol for chip-on-chip analysis. Extracted microarray intensities were processed and analyzed using the R software environment for statistical computing (http://www.r-project.org/). The data discussed in this publication have been deposited in NCBI's Gene Expression Omnibus[41] and are accessible through GEO series accession numbers GSE84028 (subseries accession numbers: GSE84018, GSE84020, GSE84021 and GSE84024).

Validation using qPCR

Gene-specific validation of MeDIP data was performed applying quantitative-real-time PCR (qPCR) (see Supplementary Table 2) using the $2^{-\Delta\Delta Ct}$ method. Data are expressed as group means ± s.e.m. To test for statistical significance, the Student's *t*-test was used (two-tailed), and the alpha level was set at 0.05.

Gene expression analysis in rats

RNA was isolated from rat PFC using AllPrep DNA/RNA Mini kit (Qiagen). RNA was analyzed by TaqMan qRT-PCR instrument (CFX384 real-time system, Bio-Rad Laboratories, Segrate, Italy) using the iScriptTM one-step RT-PCR kit for probes (Bio-Rad Laboratories) in triplicate as multiplexed reactions with a normalizing internal control (*36b4*).

Protein analysis

Protein subcellular fractionating was obtained homogenizing the tissues in a Teflon-glass potter in ice-cold 0.32 M sucrose buffer containing 1 mM HEPES, 1 mM $MgCl_2$, 1 mM $NaHCO_3$ and 0.1 mM phenylmethylsulfonyl fluoride, pH = 7.4, in the presence of a complete set of protease (Roche, Monza, Italy) and phosphatase (Sigma-Aldrich) inhibitors. Total cell homogenate was next processed to obtain the crude membrane fraction (P2) and the Triton-Insoluble post-synaptic fraction (TIF) as described in detail in the Supplementary S1 Materials and Methods.

For western blot analysis, samples were run on SDS-polyacrylamide gel electrophoresis (PAGE) and analyzed using the Chemidoc MP Imaging System after normalization on β-actin levels.

Co-immunoprecipitation assays were performed as in Vastagh *et al.*[42] with the introduction of some methodological modifications. Briefly, total cell homogenates from the rat PFC were immunoprecipitated with 3 μg of antibody overnight at 4 °C, followed by a 2 h incubation with protein A/G beads. Beads were then washed extensively and bound complexes were analyzed by SDS-PAGE and western blotting.

For all the above-mentioned molecular and biochemical analyses, all data met the assumptions of normal distribution and equality of variance.

Interaction between functional variation in Ank3 and obstetric complications on working memory processing

Association of rs9804190 with human post-mortem prefrontal Ank3 mRNA expression. Earlier results have indicated association of an intronic single-nucleotide polymorphism in the *Ank3* gene, that is rs9804190, with gene expression levels in the superior temporal gyrus of patients with schizophrenia.[28] We therefore tested such association in a large group of samples from PFC (BA46) of 268 non-psychiatric individuals using Braincloud (http://braincloud.jhmi.edu/) (Supplementary Information and Supplementary Table 3). In particular, analysis of covariance was performed, with rs9804190 genotype as the independent variable, *Ank3* mRNA expression as the dependent variable, and non-matched variables between groups (that is, age, sex, RNA integrity number) and ethnicity as covariates of no interest. A statistical threshold of $P < 0.05$ was used for this analysis.

In vivo fMRI and behavioral study

Three hundred six healthy adults (Supplementary Information and Supplementary Table 4) were enrolled in a behavioral study. One hundred seventy four of these individuals (supplementary Table 4) also participated in a functional magnetic resonance imaging (fMRI) study. In both studies, all individuals performed the 1- and 2-back versions of the N-back task, eliciting two loads of working memory (WM) processing and were genotyped for rs9804190 (Supplementary S1 Materials and Methods). Furthermore, mothers of all individuals completed the McNeil-Sjöström Scale,[43] which allowed to split individuals based on the Obstetric Complications (OC) score (Supplementary S1 Materials and Methods).[44] Sample sizes were: (a) in the fMRI sample, 57 CC with OC, 48 CC without OC, 38 T carriers with OC, 31 T carriers without OC; (b) in the behavioral study sample, 115 CC with OC, 66 CC without OC, 86 T carriers with OC, 39 T carriers without OC.

fMRI data acquisition and analysis

fMRI data were acquired with a 3T GE scanner and processed with SPM8 (see Supplementary S1 Materials and Methods). Second-level random effects multiple regression were performed to investigate *Ank3* × OC interaction on prefrontal activity during performance of the 1- and 2-back

WM tasks, using task load as the repeated-measures factor, and *Ank3* rs9804190 genotype as well as OC (absence/presence) as the between-subjects factor. We used a statistical threshold of $P < 0.05$, family-wise error small volume corrected for the left dorsolateral PFC (DLPFC), whose role is crucial in WM processing[45] and the greater involvement of the left portion of DLPFC during WM tasks eliciting both verbal and visuospatial processing.[46,47] Then, we explored the interaction between *ANK3* and OC on prefrontostriatal connectivity. With this aim, psychophysiological interaction analysis [48] was performed for each subject. In particular, we used a 5 mm region of interest centered on the peak activity ($x = -48$, $y = 38$, $z = 30$) in left DLPFC as seed region (Supplementary S1 Materials and Methods). Individual psychophysiological interaction contrasts were then entered in second-level random effects multiple regressions using task load as the repeated-measures factor, and *Ank3* rs9804190 genotype as well as OC (absence/presence) as the between-subjects factors. We used a statistical threshold of $P < 0.05$, family-wise error small-volume corrected within the left striatum (see Supplementary S1 Materials and Methods).

Analysis of behavioral data

A repeated measure factorial analysis of variance was performed, with genotype and OC presence/absence as the between-subjects factors, load (1- and 2-back) as the repeated-measures factor and behavioral accuracy (% of correct responses) or reaction time as the dependent variable. Tukey's test was used for *post hoc* analyses.

RESULTS

Genome-wide DNA methylation analyses in different paradigms of ELS exposure

MeDIP-chip analysis at PND62 in the PFC of male rats uncovered 7660 probes associated with 3475 distinct genes whose methylation status was different between control (Ctrl) and animals exposed to PNS (false discovery rate (FDR) < 0.2). In particular, 3362 probes, related to 1508 genes, were hypomethylated in PNS animals, whereas 4298 probes, corresponding to 1773 genes, were hypermethylated in PNS animals. Furthermore, the remaining 194 genes showed mixed methylation patterns. Using Ingenuity Pathway Analysis, we found enrichment for several neuronal functions, including 'psychological disorders' (Supplementary Table 5), among other important biological mechanisms.

In order to prioritize the genes that may be important in keeping the memory of the adverse perinatal experience through the regulation of their methylation status, we performed a cross-species analysis overlapping the list of genes differentially methylated in the PFC of rats exposed to PNS with the results of MeDIP-chip genome-wide analyses in two different species, humans and non-human primates, which were also characterized by exposure to adversities during the perinatal life. In the human cohort, we analyzed the methylation status of genes in $CD34^+$ hematopoietic stem cells collected from the umbilical cord of newborns from mothers with different levels of stress during gestation.[18] In addition, we used two groups of monkeys characterized by different early-life social and rearing conditions, in which we performed genome-wide analyses in the PFC of 7-year-old animals and in the peripheral T cells ($CD3^+$) at ages 30 days and 2 years, in order to look for stable peripheral DNA signatures in response to different early environmental conditions.[49,50] The analyses in monkeys, in particular, at a difference from our previously published work,[18] fill a gap as the addition of the data from the monkey PFC further integrates the results obtained at brain level (in adult rats and monkeys) with data obtained at peripheral level (in monkeys and human newborns), providing more reliability and authenticity to our trans-species approach. We identified eight genes commonly affected—regardless the direction of the methylation changes—after exposure to ELS in all the conditions described above: *Ankyrin-3* (*Ank3*), *Cyclic nucleotide gated channel alpha 4* (*Cnga4*), *Aspartyl-tRNA synthetase 2, mitochondrial* (*Dars2*), *GABA A receptor, gamma 2* (*Gabrg2*), *5-hydroxytryptamine receptor 4* (*Htr4*), *Latrophilin 2* (*Lphn2*), *Solute carrier family 22, member 2* (*Slc22a2*) and *T-cell lymphoma invasion and metastasis 1* (*Tiam1*; Figure 1). Almost all these genes showed a mixed direction of the methylation changes, with the exception of *Ank3* and *Gabrg2*, which showed a consistently higher methylation in the stressed group across all the conditions (Supplementary Table 6). *Ank3* has previously emerged as a common genetic risk factor for neurodevelopmental and psychiatric disorders, such as bipolar disorder[26,27] and schizophrenia,[28] whereas a strong dysfunction of the GABAergic system has also been demonstrated in anxiety and depression.[51,52] We focused our subsequent analyses on *Ank3* since its methylation status was affected in the same direction also in the whole blood and buccal cells from 2-year-old monkeys exposed to ELS, whereas *Gabrg2* did not (Supplementary Table 7). The extent of the methylation differences pertaining all the *Ank3* probes hypermethylated in the stressed groups is listed in Supplementary Table 8 using similar significance (*P*-values) and effect size estimates (as differential expressed in log2) as previously reported.[18,19]

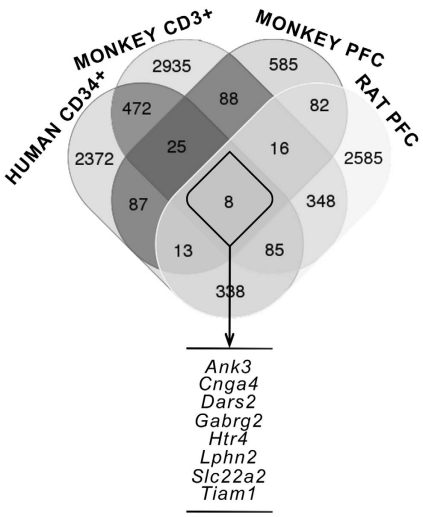

Figure 1. Venn diagram showing the overlap of the number of differentially methylated genes regulated by exposure to early-life stress in different species (see Materials and Methods for details). The eight genes listed below emerged as differentially methylated after early-life stress in all conditions. PFC, prefrontal cortex.

Validation of MeDIP-chip

We next characterized in more detail the modulation of *Ank3* in the rat model of PNS. Three genomic locations showed a different methylation status between Ctrl and PNS rats in the PFC at PND62 (Figure 2a and Supplementary Table 6). In detail, the probes located at chr20:19420344-19420403 and at chr20:19420705-19420764 were hypomethylated in PNS rats, whereas the probe located at chr20:19580638-19580697 was hypermethylated in PNS rats. qPCR analysis was used to validate the array data indicated by the arrow in Figures 2a and b, and confirmed the result obtained with MeDIP-chip (Figure 2c). We focused on this probe, as it was the only showing an increased methylation status in the stressed group, according with all the other conditions (Supplementary Tables 6 and 7).

Postnatal developmental expression of Ankyrin-3 in the PFC of male rats

Using qRT-PCR, we next examined if the altered methylation status of *Ank3* was associated with changes in its transcriptional regulation during the postnatal development until early

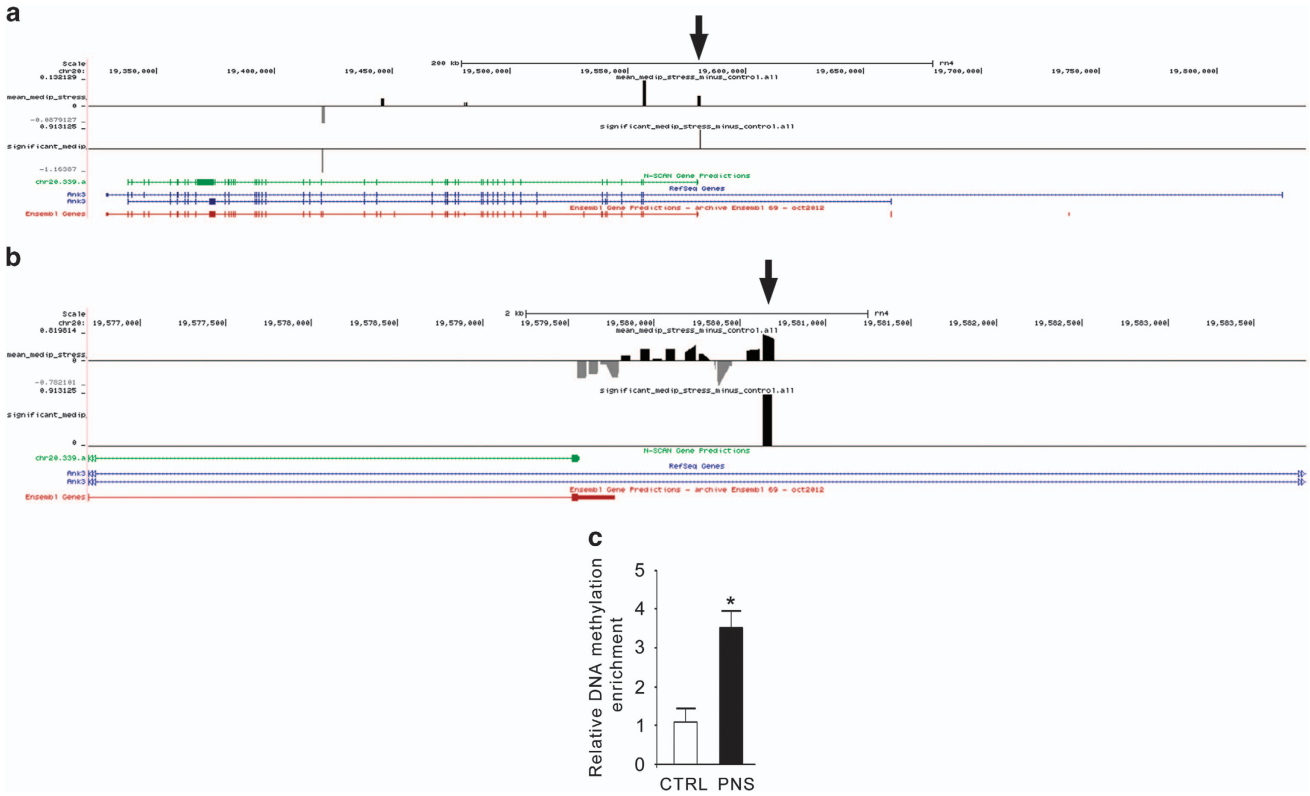

Figure 2. Expanded views from the UCSC genome browser at the rat Ank3 gene location are depicted. (**a**) The first track shows average methylation probe fold differences (Log2), whereas the second track shows the regions whose methylation status is significantly different as a consequence of PNS. The three tracks at the bottom show exons and introns boundaries taken from the rat N-SCAN Gene Predictions, NCBI Reference Sequence Database (RefSeq) and Ensembl Gene Predictions, respectively. Arrow indicates the location of DNA amplification for qPCR validation. (**b**) Zoomed view of **a** showing every single probe in the region selected for the validation in the rat prenatal stress model. (**c**) Bar graph of the qPCR validation of *Ank3* relative DNA methylation enrichment between PNS and Ctrl groups, shown as relative bound fraction concentrations. The data represent the mean ± s.e.m. of 3–4 independent determinations. *$P < 0.05$ vs Ctrl (Student's *t*-test). Ctrl, control; PNS, prenatal stress.

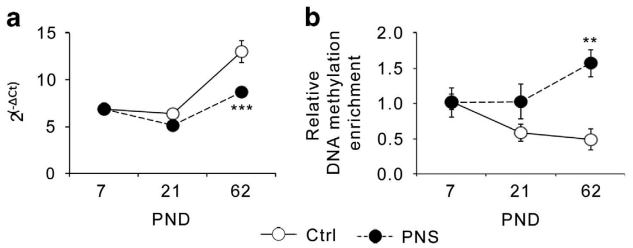

Figure 3. Exposure to prenatal stress in rats alters the DNA methylation status and the expression levels of Ank3 with a specific time-profile. (**a**) mRNA expression levels of Ankyrin-3 during the postnatal development in the prefrontal cortex of PNS male rats as compared with control animals (Ctrl). The data, expressed as fold change (where ΔCt is the difference between the threshold cycle of the target gene and the housekeeping gene) are the mean ± s.e.m. of 6–9 independent determinations. (**b**) Relative DNA methylation enrichment of Ankyrin-3 during the postnatal development in the prefrontal cortex of PNS male rats as compared with Ctrl. The data, expressed as relative bound fraction concentration, are the mean ± s.e.m. of 3–7 independent determinations. $^{**}P < 0.01$ and $^{***}P < 0.001$ vs Ctrl at the same postnatal age (2-way analysis of variance (ANOVA) followed by Fisher's LSD *post hoc* comparison). PND, postnatal day; PNS, prenatal stress.

adulthood. We found a significant effect of PNS exposure ($F_{1,41} = 14.795$, $P < 0.001$), of AGE ($F_{2,41} = 39.885$, $P < 0.001$), and a significant PNS × AGE interaction ($F_{2,41} = 7.303$, $P < 0.01$). Indeed, as depicted in Figure 3a, Ctrl rats showed a relative stable expression of *Ank3* from PND7 to PND21, followed by a steady increase at PND62, whereas PNS rats showed statistically significant lower *Ank3* mRNA levels at PND62 ($P < 0.001$), but not earlier (Figure 3a). Next, in order to establish a correlation between these changes and the epigenetic modifications at the *Ank3* gene, we investigated DNA methylation at the same gene location found to be affected using MeDIP-chip and validated with qPCR at PND62 in PNS rats. As depicted in Figure 3b, Ctrl rats showed a progressive decrease in the methylation levels of *Ank3* from PND7 to PND62, whereas PNS rats showed a stable methylation between PND7 and PND21, with a steady increase at early adulthood. Statistical analysis revealed a significant effect of PNS ($F_{1,29} = 10.315$, $P < 0.01$) and a significant PNS × AGE interaction ($F_{2,29} = 3.897$, $P < 0.05$), supporting the fact that PNS and Ctrl rats showed comparable methylation levels of *Ank3* at PND7 that progressively diverge, leading to a statistical difference at PND62 ($P < 0.01$).

Analysis of ANKG protein modulation following PNS exposure in the PFC of male rats at PND62

Ankyrin-3 encodes for a protein, ANKG, which exists in different isoforms that are expressed in nearly all tissues, although with some peculiarities. It has been recently demonstrated, for example, that the 190 kDa isoform of ANKG localizes at post-synaptic level, where it interacts with both PSD95 and GLUR1.[32] Since it has been amply demonstrated that neuropsychiatric disorders can be characterized by synaptic dysfunction,[33,34] we decided to investigate whether the long-term changes in *Ank3* expression observed in PNS animals may also involve alterations in the synaptic compartment.

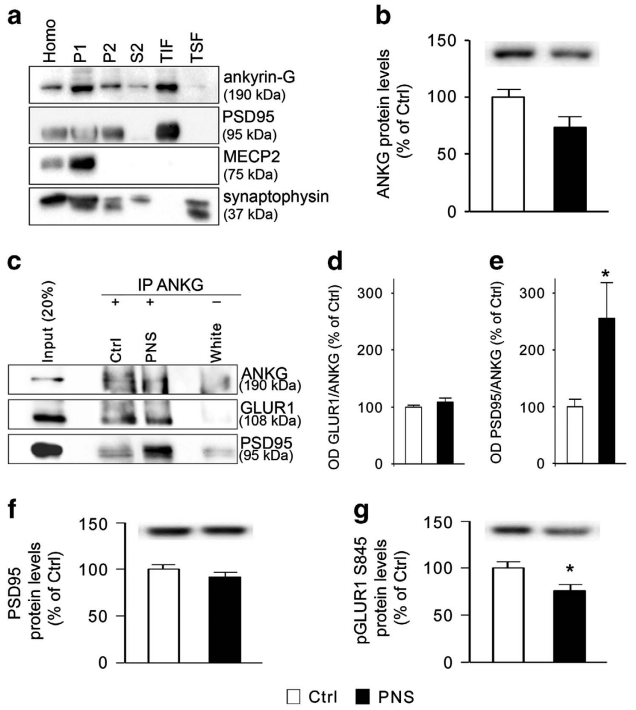

Figure 4. ANKG interaction with PSD95 and GLUR1: modulation following prenatal stress exposure in rats. (**a**) Western blot analysis of ANKG enrichment in different subcellular fractions, as compared with PSD95, MECP2 and synaptophysin. (**b**) Bar graph of ANKG protein levels in the crude membrane fraction from the prefrontal cortex of adult Ctrl and PNS male rats. (**c**) Western blot analysis of co-immunoprecipitation experiments of ANKG with GLUR1 or PSD95 from the prefrontal cortex of male rats at PND62. (**d** and **e**) Bar graph of GLUR1/ANKG (**d**) and PSD95/ANKG (**e**) interaction in the prefrontal cortex of Ctrl and PNS male rats at PND62. (**f**, **g**). Bar graphs of PSD95 (**f**) and pGLUR1 S845 (**g**) protein levels in the crude membrane fraction from the prefrontal cortex of adult Ctrl and PNS male rats. Data in bar graphs are presented as mean ± s.e.m. of 7–8 independent determinations. *$P < 0.05$ vs Ctrl (Student's *t*-test). ANKG, ankyrin-G; Homo, whole homogenate; P1, nuclear fraction; P2, crude membrane fraction; PNS, prenatal stress; S2, cytosolic fraction; TIF, triton insoluble fraction; TSF, triton soluble fraction.

Using western blot analysis, we first established the expression of ANKG 190 kDa in different subcellular fractions from the rat brain. As shown in Figure 4a, ANKG 190 kDa is enriched in the crude membrane fraction (P2) and in the TIF, which represents the post-synaptic compartment, as also occurred for the post-synaptic density marker PSD95, but not for MECP2, a marker of the nuclear compartment, or synaptophysin, a presynaptic marker (Figure 4a). Moreover, we found that ANKG 190 kDa levels were reduced by PNS in the P2 (−26% vs Ctrl, $P = 0.057$, Figure 4b).

Seen ANKG 190 kDa enrichment in the post-synaptic compartment (Figure 4a) and its trend toward a decrease in the P2 fraction (Figure 4b), we investigated, by co-immunoprecipitation assay, whether ANKG 190 kDa interacts with key molecules localized at the post-synaptic site and if PNS exposure may alter these interactions. As shown in Figure 4c, ANKG 190 kDa interacted with PSD95 as well as with GLUR1. Interestingly, we found that while GLUR1/ANKG interaction was not affected by PNS (+9% vs Ctrl, $P > 0.05$, Figure 4d), PSD95/ANKG interaction was significantly increased in the PFC of adult rats that were exposed to PNS (+155% vs Ctrl, $P < 0.05$, Figure 4e), possibly leading to alterations in the functional integrity of the post-synaptic compartment. Indeed, although we did not detect changes of PSD95 protein levels in the P2 (−13% vs Ctrl, $P > 0.05$, Figure 4f), we found a significant decrease of the phosphorylated (pS845) form of the obligatory AMPA GLUR1 subunit (−24% vs Ctrl, $P < 0.05$, Figure 4g), a proxy for receptor activation.[53]

Interaction between the Ank3 single-nucleotide polymorphism rs9804190 and OC on prefrontostriatal functional connectivity and behavior during working memory

Analysis of human post-mortem data, using the Braincloud data set,[54] indicated that the *Ank3* single-nucleotide polymorphism rs9804190 was associated with *Ank3* mRNA expression in the DLPFC ($F_{2,\ 261} = 6.66$; $P = 0.001$), with greater expression in the TT genotype as compared with CT ($P < 0.0001$) and CC ($P < 0.0001$).

We next investigated the influence of rs9804190 on brain function and the possible modulation following exposure to early-life adversities, in the form of OC. fMRI results did not indicate significant main effects of OC, of rs9804190, or their interaction on brain activity. There was a rs9804190 genotype by WM load interaction in bilateral DLPFC (Right BA9, x, y, z = 28, 40, 36; K = 68; Z score = 3.28; uncorrected $P = 0.001$. Left BA9/10, x, y, z = − 40, 46, 20; K = 60; Z score = 3.31; uncorrected $P = 0.001$). Consistent with previous studies,[28,55] CC subjects exhibited greater recruitment of bilateral PFC during 2-back compared with T carriers. On the other hand, psychophysiological interaction analysis revealed a genotype × OC × WM load interaction on functional connectivity between left DLPFC and left striatum ($x,y,z = -26, -16, 9$; $K = 111$; Z score = 3.59; family-wise error corrected $P = 0.037$). *Post hoc* analysis on values of connectivity extracted from the significant striatal cluster revealed, in presence of OC, a greater connectivity strength in T carriers as compared with CC individuals during 2-Back ($P < 0.007$; Figures 5a and b). No other statistically significant difference was found in between genotype group comparisons within each load (Tukey's HSD *post hoc* test, all $P > 0.1$).

Analysis of WM behavioral data indicated a main effect of genotype reaching significance ($F_{1.287} = 3.2$; $P = 0.07$), with greater mean values of percent correct responses in T carriers compared with CC individuals. Furthermore, there was a trend for an interaction between genotype and load ($F_{1.287} = 3.5$; $P = 0.06$], with T carrier subjects having greater mean accuracy than CC at 2-Back. No significant main effect of OC or of its interaction with WM load or rs9804190 was found (all $P > 0.1$). Notably, and similarly to the psychophysiological interaction analysis of fMRI data, there was a genotype × OC × WM load interaction on percent correct responses ($F_{1,287} = 3.88$; $P = 0.049$). More specifically, *post hoc* analysis demonstrated greater accuracy in T carriers compared with CC subjects at 2-Back in presence of OC (Tukey's HSD *post hoc* test $P = 0.0005$). No other statistically significant difference was found between genotypic group comparisons within each load (Tukey's test, all $P > 0.9$; Figure 5c). No statistically significant main effects or interaction was present on reaction time data (all $P > 0.05$).

DISCUSSION

In the present study, using a 'converging evolutionary' approach, we identified an association between the exposure to ELS and the methylation status of *Ank3* gene, which may support its role in the vulnerability to psychiatric disorders. *Ank3* methylation, mRNA and protein levels were indeed significantly altered in rats exposed to PNS with a specific temporal profile.[33] Furthermore, in humans we found an interaction between a polymorphism affecting *Ank3* expression and OC, modulating prefrontostriatal functional connectivity and behavior during WM, whose deficits are manifested in several psychiatric conditions.[37]

First, in line with previous studies showing the impact of ELS on the epigenome,[49,50,56] we found that PNS in rats persistently affected a large set of genes involved in specific biological functions. Subsequently, our cross-species, cross-tissues and

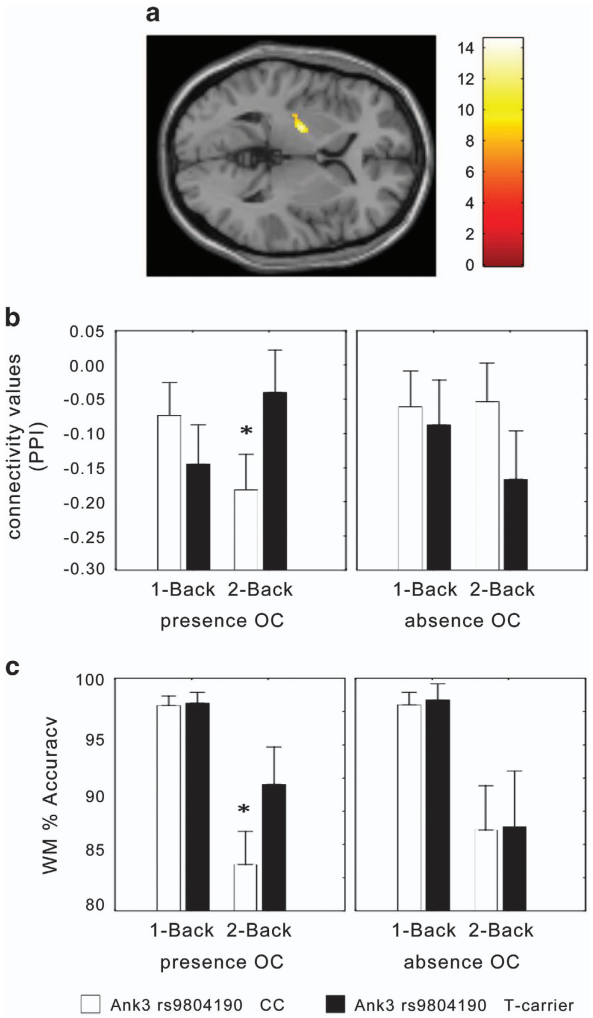

Figure 5. Healthy humans with a history of obstetric complications combined with functional variation in Ank3 gene, show altered prefrontostriatal connectivity and working memory performance. (**a**) Section of the brain depicting the left striatal cluster whose functional connection with the left DLPFC is associated with an Ank3 rs9804190 × OC interaction during WM processing. (**b**) Graph with functional connectivity values (arbitrary units) extracted from the cluster depicted in **a**. T carrier healthy subjects had greater connectivity strength compared with CC healthy individuals in the presence of OC. See text for statistics. (**c**) Graph showing an Ank3 rs9804190 × OC interaction on behavioral accuracy (% correct responses) during WM in healthy subjects. T carriers were associated with greater accuracy compared with subjects with the CC genotype (see text for statistics). DLPFC, dorsolateral prefrontal cortex; OC, Obstetric Complications; WM, working memory.

longitudinal approach pointed to the identification of eight genes whose methylation status was affected in all the investigated cohorts, which may be relevant for the long-lasting nature of the effects brought about by ELS. Although the heterogeneity of all the conditions in this study has to be taken into account (tissues, species and timing), we strongly believe that this assortment represents the strength of our experimental procedure, seeing that we, and others, already demonstrated the high validity of these convergent approaches.[18,22–24]

We found that some of the overlapping genes have not yet been previously associated with stress or psychopathology (*Cnga4*, *Dars2*, *Lphn2* and *Tiam1*). Instead, other groups have previously demonstrated an involvement of *Slc22a2* or *Htr4* in the efficacy of antidepressant medication,[57,58] whereas *Gabrg2* holds high relevance seen the involvement of GABAergic transmission in several psychiatric disorders.[51,59]

Seen the concordance of the methylation changes across all the conditions and species investigated in the present study, we decided to focus our attention on *Ank3*, which is among the most consistently replicated and statistically significant genetic risk factor for neuropsychiatric diseases.[25–28,30]

In the adult PFC from PNS rats, we detected an increase in DNA methylation in the first intron of *Ank3*, although we also found two differentially methylated regions downstream, within intron 24, which were more methylated in Ctrl rats. Interestingly, this same location was also found to be hypermethylated in the hippocampus of PNS male rats compared with Ctrl (chr20.19580650-19580709, FDR = 0.006), an effect that we validated also at mRNA level (Ctrl: 100 ± 8 and PNS: 77 ± 7, $P < 0.05$), as in the PFC. Although hypermethylation within a promoter is frequently correlated with transcriptional silencing,[60–62] it has been also shown that hypermethylated promoters could be activated in a transient way through chromatin remodeling, without demethylation[63] and, on the contrary, that the promoter hypomethylation does not necessarily correlate with active transcription, as other epigenetic mechanisms could act in concert to repress gene expression.[64] Moreover, although DNA methylation of CpG islands associated to promoter regions has been amply investigated, several studies, including our own, have shown that also intragenic and intronic regions are widely modulated after environmental stressors through methylation, thus affecting transcriptional regulation using different mechanisms, such as alternative splicing rather than alternative promoters.[62,65] Indeed, we showed that PNS rats have decreased total mRNA levels of *Ank3* at PND62 as a function of different methylation levels at this genomic location. Several studies, at least in mice, have shown the complexity of *Ank3* gene organization and the existence of different mRNA isoforms with a specific tissue and cellular localization and function,[66] and based on NCBI Genbank, rats seems to share a similar transcriptional organization to mice and humans. However, in this work, using qRT-PCR, we evaluated the total mRNA levels of *Ank3*, as the differentially methylated region is within a locus included in all *Ank3* rat mRNA transcript variants. We found that *Ank3* mRNA levels are relatively stable before weaning, with a steep increase thereafter to reach adult expression, suggesting a role for *Ank3* across the postnatal neurodevelopment and in the impending maturational steps, as already hypothesized.[67–69] Conversely, the shift between weaning and adulthood is affected in PNS rats, leading to a significant reduction of *Ank3* expression at adulthood. Interestingly, we have recently shown that the expression of *Bdnf*, a neurotrophin involved in psychiatric disorders, is significantly downregulated in PNS rats only after adolescence,[39] thus supporting the idea that exposure to ELS may influence life-long genome adaptation thus resulting in behavioral disorders, such as bipolar disorder, depression and schizophrenia, that frequently become manifest during adolescence.[13,70–72]

Indeed, ELS can affect the epigenome in a persistent manner.[18,73–75] However, it is not clear whether DNA methylation changes represent a direct consequence of the early-life experiences or a result of the psychopathological phenotype associated with perinatal adversities. We demonstrated that PNS animals not only failed to show a progressive decrease in the DNA methylation levels of *Ank3* as occurring in Ctrl, but they displayed a gradual increase after weaning. It may be inferred that two concomitant events may lead to a reduction of *Ank3* expression from weaning to adulthood: a failure of the mechanisms that reduce gene methylation (as occurring in Ctrl rats), together with an activation of *de novo* methylation as long-term consequence of stress exposure. Similar to these findings, Weaver and colleagues have previously demonstrated that maternal behavior alters the methylation status of the glucocorticoid receptor during the first

week of life, thus affecting its expression in the hippocampus until adulthood.[76]

We also showed that exposure to PNS led to functional alterations in the protein encoded by *Ank3* gene, namely ANKG. We found that ANKG is enriched in the membrane compartment (P2 and TIF), as previously demonstrated using primary cortical neurons,[32] and that PNS may affect its subcellular distribution reducing its protein levels selectively in this fraction (compartment). Furthermore, we showed that the interaction of ANKG with PSD95 was significantly increased in PNS animals, which may alter the functional integrity of the post-synaptic domain. As an example, Yaka *et al*.[77] demonstrated that a mild form of PNS determined an increase of synaptic PSD95 levels in the hippocampus in juvenile rats, thus altering glutamate receptor clustering and leading to impairments in LTP and memory tasks. Even if we failed to detect changes of PSD95 protein levels in PNS animals, the abnormal interaction of PSD95 with ANKG 190 kDa could contribute to a disrupted AMPAR clustering and function, as also demonstrated by the reduction of the phosphorylation levels of GLUA1 S845 in PNS rats, a proxy for receptor activation.[53] As the glutamatergic synapse represents a key player in the pathogenesis and development of neuropsychiatric disorders,[33,34] our data suggest that ANKG may mediate some of the detrimental effects of PNS exposure on the glutamatergic architecture.

Furthermore, we provided evidence for a functional outcome of reduced *Ank3* expression in humans. Indeed, by investigating an *Ank3* single-nucleotide polymorphism, rs9804190, which has previously been associated with heightened risk for different psychiatric disorders,[27,28,78,79,80] we found that the C allele predicts lower post-mortem prefrontal *Ank3* expression in non-psychiatric subjects. Interestingly, CC subjects with OC had lower prefrontostriatal functional connectivity strength and lower behavioral accuracy at the higher WM demand, as compared with T carriers with OC. These results suggest that a genetic context leading to lower *Ank3* expression interacts with the presence of OC, a relevant factor of early stress, in determining sub-optimal patterns of brain functional connections and behavior during WM. Some limitations of our study need to be considered. First, the relatively small sample size in the MeDIP studies, which is due to technical issues. Second, for the animal cohorts (both rats and monkeys) only males have been used, which could limit the conclusions to a sex-specific effect. Seen the existence of sex bias in the prevalence and severity of many neurodevelopmental and psychiatric disorders, and evidence suggesting that environment has a sex-dependent effect on DNA methylation itself,[81,82] future studies are needed to investigate whether such alterations may characterize also the female counterpart. It is also important to mention that following ELS the methylation differences across species occur in different regions, whose functional impact on gene function remains to be established. Last, although we limited the analysis to the PFC for performing cross-species investigation, we cannot rule out the possibility that methylation changes in other key brain regions, such as the hippocampus and the basal ganglia, may mediate the long-term effect of ELS on the susceptibility to psychopathology.

The results in humans at the imaging and behavioral level, together with those obtained by our methylation analysis, suggest that *Ank3* may represent an important link between ELS and the development of psychopathology, through alterations in neuronal circuits relevant for psychiatric diseases. Moreover, given the possibility that *Ank3* expression can be modulated by pharmacological intervention [31] and that the behavioral phenotype induced by *Ank3* suppression in the mouse brain may be reverted by chronic lithium administration,[83] we believe that *Ank3* may represent a novel molecular marker as well as a target for drug intervention in stress-related disorders with a neurodevelopmental origin.

CONFLICT OF INTEREST

MAR reports having received compensation as speaker/consultant from Lundbeck, Otzuka, Sumitomo Dainippon Pharma, Sunovion and Takeda. A Bertolino disclosed consulting fees from Hoffman-La Roche. The remaining authors declare no conflict of interest.

ACKNOWLEDGMENTS

This work was supported by an ERANET Neuron grant to MD, MS, MAR and PG, as well as by grants from the Italian Ministry of University and Research to MAR (PRIN – grant number 20107MSMA4_002) and from Fondazione CARIPLO (grant number 2012-0503) to MAR, FC and A Bertolino. In addition, characterization of the human cohort was supported by a grant of the Dietmar Hopp Foundation. VN received support from the Olympia-Morata-Programme of the University of Heidelberg and the Boehringer-Ingelheim Fonds. AL was supported by a Fondazione Umberto Veronesi Fellowship. ZN was supported by Marie Curie International Outgoing Fellowship within the 7th European Community Framework Programme. Work in MS's laboratory was supported by Canadian Institute of Health Research Grant MOP-42411. We are grateful to Elisa Zianni and Dr Jennifer Stanic for the help with co-immunoprecipitation.

REFERENCES

1 Barker DJ. Intrauterine programming of adult disease. *Mol Med Today* 1995; **1**: 418–423.
2 Weinstock M. The long-term behavioural consequences of prenatal stress. *Neurosci Biobehav Rev* 2008; **32**: 1073–1086.
3 Lupien SJ, McEwen BS, Gunnar MR, Heim C. Effects of stress throughout the lifespan on the brain, behaviour and cognition. *Nat Rev Neurosci* 2009; **10**: 434–445.
4 Kolb B, Mychasiuk R, Muhammad A, Li Y, Frost DO, Gibb R. Experience and the developing prefrontal cortex. *Proc Natl Acad Sci USA* 2012; **109**(Suppl 2): 17186–17193.
5 Provencal N, Binder EB. The neurobiological effects of stress as contributors to psychiatric disorders: focus on epigenetics. *Curr Opin Neurobiol* 2015; **30**: 31–37.
6 Gudsnuk K, Champagne FA. Epigenetic influence of stress and the social environment. *ILAR J* 2012; **53**: 279–288.
7 Zhang TY, Meaney MJ. Epigenetics and the environmental regulation of the genome and its function. *Ann Rev Psychol* 2010; **61**: c431–c433.
8 Klengel T, Pape J, Binder EB, Mehta D. The role of DNA methylation in stress-related psychiatric disorders. *Neuropharmacology* 2014; **80**: 115–132.
9 Szyf M. The genome- and system-wide response of DNA methylation to early life adversity and its implication on mental health. *Can J Psychiatry* 2013; **58**: 697–704.
10 Babenko O, Kovalchuk I, Metz GA. Stress-induced perinatal and transgenerational epigenetic programming of brain development and mental health. *Neurosci Biobehav Rev* 2015; **48**: 70–91.
11 Maccari S, Krugers HJ, Morley-Fletcher S, Szyf M, Brunton PJ. The consequences of early-life adversity: neurobiological, behavioural and epigenetic adaptations. *J Neuroendocrinol* 2014; **26**: 707–723.
12 Meaney MJ, Szyf M. Maternal care as a model for experience-dependent chromatin plasticity? *Trends Neurosci* 2005; **28**: 456–463.
13 Provencal N, Binder EB. The effects of early life stress on the epigenome: From the womb to adulthood and even before. *Exp Neurol* 2015; **268**: 10–20.
14 Worlein JM. Nonhuman primate models of depression: effects of early experience and stress. *ILAR J* 2014; **55**: 259–273.
15 Nishi M, Horii-Hayashi N, Sasagawa T. Effects of early life adverse experiences on the brain: implications from maternal separation models in rodents. *Front Neurosci* 2014; **8**: 166.
16 Guidotti A, Dong E, Tueting P, Grayson DR. Modeling the molecular epigenetic profile of psychosis in prenatally stressed mice. *Prog Mol Biol Transl Sci* 2014; **128**: 89–101.
17 Darnaudery M, Maccari S. Epigenetic programming of the stress response in male and female rats by prenatal restraint stress. *Brain Res Rev* 2008; **57**: 571–585.
18 Nieratschker V, Massart R, Gilles M, Luoni A, Suderman MJ, Krumm B *et al.* MORC1 exhibits cross-species differential methylation in association with early life stress as well as genome-wide association with MDD. *Transl Psychiatry* 2014; **4**: e429.
19 Provencal N, Suderman MJ, Guillemin C, Massart R, Ruggiero A, Wang D *et al.* The signature of maternal rearing in the methylome in rhesus macaque prefrontal cortex and T cells. *J Neurosci* 2012; **32**: 15626–15642.
20 Kaufman IC, Rosenblum LA. Effects of separation from mother on the emotional behavior of infant monkeys. *Ann N Y Acad Sci* 1969; **159**: 681–695.
21 Bock J, Wainstock T, Braun K, Segal M. Stress in utero: prenatal programming of brain plasticity and cognition. *Biol Psychiatry* 2015; **6**: 00162–00166.

22 Bertsch B, Ogden CA, Sidhu K, Le-Niculescu H, Kuczenski R, Niculescu AB. Convergent functional genomics: a Bayesian candidate gene identification approach for complex disorders. *Methods* 2005; **37**: 274–279.
23 Le-Niculescu H, Balaraman Y, Patel SD, Ayalew M, Gupta J, Kuczenski R *et al.* Convergent functional genomics of anxiety disorders: translational identification of genes, biomarkers, pathways and mechanisms. *Transl Psychiatry* 2011; **1**: e9.
24 Schmidt M, Brandwein C, Luoni A, Sandrini P, Calzoni T, Deuschle M *et al.* Morc1 knockout evokes a depression-like phenotype in mice. *Behav Brain Res* 2015; **296**: 7–14.
25 Iqbal Z, Vandeweyer G, van der Voet M, Waryah AM, Zahoor MY, Besseling JA *et al.* Homozygous and heterozygous disruptions of ANK3: at the crossroads of neurodevelopmental and psychiatric disorders. *Hum Mol Genet* 2013; **22**: 1960–1970.
26 Ferreira MA, O'Donovan MC, Meng YA, Jones IR, Ruderfer DM, Jones L *et al.* Collaborative genome-wide association analysis supports a role for ANK3 and CACNA1C in bipolar disorder. *Nat Genet* 2008; **40**: 1056–1058.
27 Schulze TG, Detera-Wadleigh SD, Akula N, Gupta A, Kassem L, Steele J *et al.* Two variants in Ankyrin 3 (ANK3) are independent genetic risk factors for bipolar disorder. *Mol Psychiatry* 2009; **14**: 487–491.
28 Roussos P, Katsel P, Davis KL, Bitsios P, Giakoumaki SG, Jogia J *et al.* Molecular and genetic evidence for abnormalities in the nodes of Ranvier in schizophrenia. *Arch Gen Psychiatry* 2012; **69**: 7–15.
29 Komada M, Soriano P. [Beta]IV-spectrin regulates sodium channel clustering through ankyrin-G at axon initial segments and nodes of Ranvier. *J Cell Biol* 2002; **156**: 337–348.
30 Sklar PR S, Scott, L J, Andreassen, O A, Cichon S, Craddock N *et al.* Large-scale genome-wide association analysis of bipolar disorder identifies a new susceptibility locus near ODZ4. *Nat Genet* 2011; **43**: 977–983.
31 Nanavati D, Austin DR, Catapano LA, Luckenbaugh DA, Dosemeci A, Manji HK *et al.* The effects of chronic treatment with mood stabilizers on the rat hippocampal post-synaptic density proteome. *J Neurochem* 2011; **119**: 617–629.
32 Smith KR, Kopeikina KJ, Fawcett-Patel JM, Leaderbrand K, Gao R, Schurmann B *et al.* Psychiatric risk factor ANK3/ankyrin-G nanodomains regulate the structure and function of glutamatergic synapses. *Neuron* 2014; **84**: 399–415.
33 de Bartolomeis A, Latte G, Tomasetti C, Iasevoli F. Glutamatergic postsynaptic density protein dysfunctions in synaptic plasticity and dendritic spines morphology: relevance to schizophrenia and other behavioral disorders pathophysiology, and implications for novel therapeutic approaches. *Mol Neurobiol* 2014; **49**: 484–511.
34 Duman RS, Aghajanian GK. Synaptic dysfunction in depression: potential therapeutic targets. *Science* 2012; **338**: 68–72.
35 Focking M, Lopez LM, English JA, Dicker P, Wolff A, Brindley E *et al.* Proteomic and genomic evidence implicates the postsynaptic density in schizophrenia. *Mol Psychiatry* 2015; **20**: 424–432.
36 Penzes P, Cahill ME, Jones KA, VanLeeuwen JE, Woolfrey KM. Dendritic spine pathology in neuropsychiatric disorders. *Nat Neurosci* 2011; **14**: 285–293.
37 Bertolino A, Blasi G. The genetics of schizophrenia. *Neuroscience* 2009; **164**: 288–299.
38 Maccari S, Piazza PV, Kabbaj M, Barbazanges A, Simon H, Le Moal M. Adoption reverses the long-term impairment in glucocorticoid feedback induced by prenatal stress. *J Neurosci* 1995; **15**(1 Pt 1): 110–116.
39 Luoni A, Berry A, Calabrese F, Capoccia S, Bellisario V, Gass P *et al.* Delayed BDNF alterations in the prefrontal cortex of rats exposed to prenatal stress: preventive effect of lurasidone treatment during adolescence. *Eur Neuropsychopharmacol* 2014; **24**: 986–995.
40 Faul F, Erdfelder E, Lang AG, Buchner A. G*Power 3: a flexible statistical power analysis program for the social, behavioral, and biomedical sciences. *Behav Res Methods* 2007; **39**: 175–191.
41 Edgar R, Domrachev M, Lash AE. Gene Expression Omnibus: NCBI gene expression and hybridization array data repository. *Nucleic Acids Res* 2002; **30**: 207–210.
42 Vastagh C, Gardoni F, Bagetta V, Stanic J, Zianni E, Giampa C *et al.* N-methyl-D-aspartate (NMDA) receptor composition modulates dendritic spine morphology in striatal medium spiny neurons. *J Biol Chem* 2012; **287**: 18103–18114.
43 McNeil TF, Cantor-Graae E, Sjostrom K. Obstetric complications as antecedents of schizophrenia: empirical effects of using different obstetric complication scales. *J Psychiatr Res* 1994; **28**: 519–530.
44 Verdoux H, Sutter AL. Perinatal risk factors for schizophrenia: diagnostic specificity and relationships with maternal psychopathology. *Am J Med Genet* 2002; **114**: 898–905.
45 Callicott JH, Mattay VS, Bertolino A, Finn K, Coppola R, Frank JA *et al.* Physiological characteristics of capacity constraints in working memory as revealed by functional MRI. *Cereb Cortex* 1999; **9**: 20–26.
46 Rottschy C, Langner R, Dogan I, Reetz K, Laird AR, Schulz JB *et al.* Modelling neural correlates of working memory: a coordinate-based meta-analysis. *Neuroimage* 2012; **60**: 830–846.
47 Wager TD, Smith EE. Neuroimaging studies of working memory: a meta-analysis. *Cogn Affect Behav Neurosci* 2003; **3**: 255–274.
48 Friston KJ, Buechel C, Fink GR, Morris J, Rolls E, Dolan RJ. Psychophysiological and modulatory interactions in neuroimaging. *Neuroimage* 1997; **6**: 218–229.
49 Massart R, Suderman M, Provencal N, Yi C, Bennett AJ, Suomi S *et al.* Hydroxymethylation and DNA methylation profiles in the prefrontal cortex of the non-human primate rhesus macaque and the impact of maternal deprivation on hydroxymethylation. *Neuroscience* 2014; **268**: 139–148.
50 Nemoda Z, Massart R, Suderman M, Hallett M, Li T, Coote M *et al.* Maternal depression is associated with DNA methylation changes in cord blood T lymphocytes and adult hippocampi. *Transl Psychiatry* 2015; **5**: e545.
51 Luscher B, Shen Q, Sahir N. The GABAergic deficit hypothesis of major depressive disorder. *Molecular psychiatry* 2011; **16**: 383–406.
52 Smith KS, Rudolph U. Anxiety and depression: mouse genetics and pharmacological approaches to the role of GABA(A) receptor subtypes. *Neuropharmacology* 2012; **62**: 54–62.
53 Wang JQ, Arora A, Yang L, Parelkar NK, Zhang G, Liu X *et al.* Phosphorylation of AMPA receptors: mechanisms and synaptic plasticity. *Molecular neurobiology* 2005; **32**: 237–249.
54 Colantuoni C, Lipska BK, Ye T, Hyde TM, Tao R, Leek JT *et al.* Temporal dynamics and genetic control of transcription in the human prefrontal cortex. *Nature* 2011; **478**: 519–523.
55 Delvecchio G, Dima D, Frangou S. The effect of ANK3 bipolar-risk polymorphisms on the working memory circuitry differs between loci and according to risk-status for bipolar disorder. *Am J Med Genet B Neuropsychiatr Genet* 2015; **168b**: 188–196.
56 Cao-Lei L, Massart R, Suderman MJ, Machnes Z, Elgbeili G, Laplante DP *et al.* DNA methylation signatures triggered by prenatal maternal stress exposure to a natural disaster: Project Ice Storm. *PLoS One* 2014; **9**: e107653.
57 Bacq A, Balasse L, Biala G, Guiard B, Gardier AM, Schinkel A *et al.* Organic cation transporter 2 controls brain norepinephrine and serotonin clearance and antidepressant response. *Mol Psychiatry* 2012; **17**: 926–939.
58 Lucas G, Rymar VV, Du J, Mnie-Filali O, Bisgaard C, Manta S *et al.* Serotonin(4) (5-HT(4)) receptor agonists are putative antidepressants with a rapid onset of action. *Neuron* 2007; **55**: 712–725.
59 Schmidt MJ, Mirnics K. Neurodevelopment, GABA system dysfunction, and schizophrenia. *Neuropsychopharmacology* 2015; **40**: 190–206.
60 Stein R, Razin A, Cedar H. In vitro methylation of the hamster adenine phosphoribosyltransferase gene inhibits its expression in mouse L cells. *Proc Natl Acad Sci USA* 1982; **79**: 3418–3422.
61 Illingworth RS, Bird AP. CpG islands--'a rough guide'. *FEBS Lett* 2009; **583**: 1713–1720.
62 Kulis M, Queiros AC, Beekman R, Martin-Subero JI, Intragenic DNA. methylation in transcriptional regulation, normal differentiation and cancer. *Biochim Biophys Acta* 2013; **1829**: 1161–1174.
63 Raynal NJ, Si J, Taby RF, Gharibyan V, Ahmed S, Jelinek J *et al.* DNA methylation does not stably lock gene expression but instead serves as a molecular mark for gene silencing memory. *Cancer Res* 2012; **72**: 1170–1181.
64 Cao R, Wang L, Wang H, Xia L, Erdjument-Bromage H, Tempst P *et al.* Role of histone H3 lysine 27 methylation in Polycomb-group silencing. *Science* 2002; **298**: 1039–1043.
65 Nagy C, Suderman M, Yang J, Szyf M, Mechawar N, Ernst C *et al.* Astrocytic abnormalities and global DNA methylation patterns in depression and suicide. *Mol Psychiatry* 2015; **20**: 320–328.
66 Kordeli E, Lambert S, Bennett V. AnkyrinG. A new ankyrin gene with neural-specific isoforms localized at the axonal initial segment and node of Ranvier. *J Biol Chem* 1995; **270**: 2352–2359.
67 Birnbaum R, Jaffe AE, Hyde TM, Kleinman JE, Weinberger DR. Prenatal expression patterns of genes associated with neuropsychiatric disorders. *Am J Psychiatry* 2014; **171**: 758–767.
68 Durak O, de Anda FC, Singh KK, Leussis MP, Petryshen TL, Sklar P *et al.* Ankyrin-G regulates neurogenesis and Wnt signaling by altering the subcellular localization of beta-catenin. *Mol Psychiatry* 2015; **20**: 388–397.
69 Talkowski ME, Rosenfeld JA, Blumenthal I, Pillalamarri V, Chiang C, Heilbut A *et al.* Sequencing chromosomal abnormalities reveals neurodevelopmental loci that confer risk across diagnostic boundaries. *Cell* 2012; **149**: 525–537.
70 Paus T, Keshavan M, Giedd JN. Why do many psychiatric disorders emerge during adolescence? *Nat Rev Neurosci* 2008; **9**: 947–957.
71 Dobbs D. Schizophrenia: The making of a troubled mind. *Nature* 2010; **468**: 154–156.
72 Szyf M. Implications of a life-long dynamic epigenome. *Epigenomics* 2009; **1**: 9–12.
73 Klengel T, Mehta D, Anacker C, Rex-Haffner M, Pruessner JC, Pariante CM *et al.* Allele-specific FKBP5 DNA demethylation mediates gene-childhood trauma interactions. *Nat Neurosci* 2013; **16**: 33–41.

74 McGowan PO, Sasaki A, D'Alessio AC, Dymov S, Labonte B, Szyf M *et al.* Epigenetic regulation of the glucocorticoid receptor in human brain associates with childhood abuse. *Nat Neurosci* 2009; **12**: 342–348.
75 Bale TL. Epigenetic and transgenerational reprogramming of brain development. *Nat Rev Neurosci* 2015; **16**: 332–344.
76 Weaver IC, Cervoni N, Champagne FA, D'Alessio AC, Sharma S, Seckl JR *et al.* Epigenetic programming by maternal behavior. *Nature neuroscience* 2004; **7**: 847–854.
77 Yaka R, Salomon S, Matzner H, Weinstock M. Effect of varied gestational stress on acquisition of spatial memory, hippocampal LTP and synaptic proteins in juvenile male rats. *Behav Brain Res* 2007; **179**: 126–132.
78 Logue MW, Solovieff N, Leussis MP, Wolf EJ, Melista E, Baldwin C *et al.* The ankyrin-3 gene is associated with posttraumatic stress disorder and externalizing comorbidity. *Psychoneuroendocrinology* 2013; **38**: 2249–2257.
79 Linke J, Witt SH, King AV, Nieratschker V, Poupon C, Gass A *et al.* Genome-wide supported risk variant for bipolar disorder alters anatomical connectivity in the human brain. *Neuroimage* 2012; **59**: 3288–3296.
80 Tesli M, Koefoed P, Athanasiu L, Mattingsdal M, Gustafsson O, Agartz I *et al.* Association analysis of ANK3 gene variants in nordic bipolar disorder and schizophrenia case-control samples. *Am J Med Genet B Neuropsychiatr Genet* 2011; **156B**: 969–974.
81 Liu J, Morgan M, Hutchison K, Calhoun VD. A study of the influence of sex on genome wide methylation. *PloS one* 2010; **5**: e10028.
82 van Dongen J, Nivard MG, Willemsen G, Hottenga JJ, Helmer Q, Dolan CV *et al.* Genetic and environmental influences interact with age and sex in shaping the human methylome. *Nat Commun* 2016; **7**: 11115.
83 Leussis MP, Berry-Scott EM, Saito M, Jhuang H, de Haan G, Alkan O *et al.* The ANK3 bipolar disorder gene regulates psychiatric-related behaviors that are modulated by lithium and stress. *Biol Psychiatry* 2013; **73**: 683–690.

Supplementary Information accompanies the paper on the Translational Psychiatry website (http://www.nature.com/tp)

SUPPLEMENTARY DETAILED METHODS

Human cohort for MeDIP-chip analysis

Subjects

The human cohort of mothers and their infants (n=180) has been recruited between 03/2011 and 03/2012 from two obstetric hospitals in the Rhine-Neckar Region of Germany (Mannheim, Ludwigshafen). The mothers were recruited during the third trimester of pregnancy (i.e. 4-8 weeks prior to delivery). Inclusion criteria for mothers were: Caucasian descent; main caregiver; German-speaking; and age 16 – 40 years. Exclusion criteria were: maternal hepatitis B, hepatitis C or HIV-infection; any current psychiatric disorders requiring inpatient treatment; a history, current diagnosis, of schizophrenia / psychotic disorder, or any substance dependence other than nicotine during pregnancy. Exclusion criteria for infants were: birth weight < 1 500 grams; gestational age at birth < 32 week; multiples; or any congenital diseases; malformations; deformations or chromosomal abnormality. The study protocol was approved by the Ethics Committee of the Medical Faculty Mannheim of the University of Heidelberg, and the study was conducted in accordance with the Declaration of Helsinki. All mothers provided written informed consent prior to participation.

Assessment of exposure to stress during the third trimester of gestation and selection of samples for the genome-wide methylome analysis

The mothers were assessed using a structured interview and a series of questionnaires in order to collect information concerning a broad range of environmental and socio-demographic risk factors, prenatal medical risk factors, general medical characteristics, and psychosocial risk factors (see supplementary

Table 1a for a summary of this phenotypic assessment). Cord blood was collected immediately after birth. Eight main stressor variables derived from eight different questionnaires were selected to represent a variety of prenatal adversities, and to take three different dimensions of stress into account: a) maternal psychopathology (primarily depressive and anxiety symptoms); b) perceived stress; c) socioeconomic and psychosocial stress (for details see supplementary Table 1b). In addition, an "adversity score" was calculated by summing up the number of dichotomous stressful prenatal adverse conditions and environmental circumstances (for details see supplementary Table 1b). To obtain a homogeneous composite measure of prenatal stress, a principal component analysis (PCA) was performed. This involved the eight main stressor variables and the total adversity score as a ninth main variable. This analysis yielded a first principal component (PC1), which explained around 60% of the common variance. PC1 was then used to determine the following two extreme groups: 10 infants with extremely high levels of prenatal ELS and 10 infants with extremely low levels of prenatal ELS.

The socio-demographic and medical characteristics of the mothers and infants in the extreme groups are shown in supplementary Table 1c. The psychopathology, perceived stress, and psychosocial and socioeconomic stress status of the mothers are shown in supplementary Table 1b. For the comparison of the extreme groups, two-tailed *t*-tests for independent samples were used (SPSS® Statistics 20). The nominal level of significance was set at $\alpha = 0.05$. All data and results are expressed as means ± standard deviation (SD) or as a percentage, as appropriate. The epigenome data sets of two infants in the low ELS group did not pass our quality control filters, and the group size decreased to n = 8.

Animals and experimental paradigms

Monkeys and rearing procedures

Prefrontal cortices (PFC), whole blood, CD3+ and buccal samples were obtained from rhesus monkeys (*Macaca mulatta*), randomly divided into two groups at birth resulting in different early life social and rearing experience, as previously described [1,2]. In detail, the "mother-reared" (MR) monkeys were raised by their biological mother in a social group, whereas "surrogate peer-reared" (SPR) monkeys were reared with an inanimate surrogate as well as daily socialization periods with age-mate peers. For the first month of life, the SPR monkeys were placed in a nursery until they were able to drink milk from a bottle by themselves at which point they were transferred to a cage with their surrogate mother. At approximately 7 months of age, animals were socially housed in large, mixed sex peer groups. PFC samples were obtained from 7-year-old male monkeys [2]. Venous blood samples were obtained from 30 days old and 2-years old monkeys at their routine medical check-up under chemical restrain (using ketamine), in order to look for stable peripheral DNA signals in response to different early environmental conditions [3,4]. Whole blood and buccal swab samples were taken at 2 years or older age. The use of experimental animals was approved by the Institutional Animal Care and Use Committee of the NICHD. All animal experiments were carried out in accordance with the National Institute of Health Guide for the Care and Use of Laboratory Animals. All efforts were made to minimize animal suffering and to reduce the number of animals used.

Rats and prenatal stress exposure

Nulliparous adult female (body weight 230–260 g) and male (400 g) Sprague-Dawley rats were purchased from a commercial breeder (Charles River, Calco, Italy). Upon arrival, they were pair-housed with a same-sex conspecific with food and water available *ad libitum* (21±1 °C, 60±10% relative humidity, regular 12/12 h light/dark cycle).

After 10 days of habituation in the facility, rats were mated for 24 h and individually housed immediately thereafter. Pregnant females were randomly assigned to control (Ctrl) or prenatal stress (PNS) conditions, as previously described [1,5,6]. In particular, PNS consisted of restraining pregnant dams in a transparent Plexiglas cylinder (7.5 cm diameter, 19 cm length) under bright light for 45 min three times daily during the last week of gestation until delivery. PNS sessions were separated by 2–3 h intervals and conducted at varying periods of the day in order to reduce habituation. Control rats were left undisturbed.

On postnatal day (PND) 1, pups from Ctrl and PNS dams were weighted, and litters were culled to 5 males and 5 females. Weaning occurred on PND21 and same sex rats were housed in groups of 3 per cage. At PND7, PND21 and PND62 one male pertaining to each litter was sacrificed.

All animal experiments were conducted according to the authorization from the Health Ministry n. 295/2012-A (20/12/2012), in full accordance with the Italian legislation on animal experimentation (D.L. 116/92) and adherent to EU recommendation (EEC Council Directive 86/609). All efforts were made to minimize animal suffering and to reduce the total number of animals used, while maintaining statistically valid group numbers.

Molecular analyses

Separation of CD34+ cells from human cord blood and extraction of genomic DNA

Human cord blood was drawn into ethylenediaminetetraacetic acid (EDTA) coated tubes immediately after birth. CD34+ cells were extracted within 24 h following delivery. Briefly, peripheral blood mononuclear cells (PBMC) were isolated by centrifuging the cord blood with Ficoll-Paque PLUS (GE Healthcare, Munich, Germany) in Leucosep tubes (Greiner Bio-One, Frickenhausen, Germany). CD34+ cells were then isolated from the PBMCs by immunomagnetic isolation using the Dynal CD34 Progenitor Cell Selection System (Life Technologies, Darmstadt, Germany) in accordance with the manufacturer´s instructions. The CD34+ cells were then stored at −80°C until DNA extraction. DNA was extracted from CD34+ cells using the Qiagen Blood Mini Kit (Qiagen, Hilden, Germany) in accordance with the instructions of the manufacturer.

Prefrontal cortex dissection and DNA preparation from monkeys

Animals were sedated with ketamine and brought to a deep surgical plane of anesthesia with pentobarbital administered intravenously, given to effect. A craniotomy was performed, followed by a thoracotomy and perfusion through the left ventricle of the heart for 1.5 min with a chilled, oxygenated buffer solution. The brain was then removed within 5 min and the prefrontal cortices (PFC) were flash frozen in isopentane at -55°C within 15 min of death and kept at -80°C until later analyses. The tissue consisted mostly of DLPFC and ventro-lateral PFC rostral to the caudal end of the arcuate sulcus, dorsal to the cingulate sulcus and lateral to the lateral orbital sulcus. PFC DNA was extracted using the Qiagen DNeasy kit following the protocol of the manufacturer.

Whole blood samples and buccal cell collection from monkeys

A small fraction (0.3 ml) of the peripheral venous blood collected for T cell isolation was used for DNA isolation with the Wizard Genomic DNA Purification kit (Promega, Madison, WI, USA) following the instructions of the manufacturer. At the same medical check-up (when the monkeys were under chemical restrain) buccal cells were collected by rubbing the inner cheeck or gum with swabs 3 times. The 3 swabs were stored in one tube at −20°C until the DNA isolation, which started with 1 hour of incubation with 60 µg proteinase K in the Nuclei Lysis Solution of the Wizard Genomic DNA Purification kit.

Separation of CD3+ T cells from monkey peripheral blood

For the CD3+ T cell separation, 20 ml of peripheral blood was drawn into EDTA-coated tubes from the 2-year old monkeys and stored at 4°C overnight. From 30-day old monkeys, 3 ml of blood was perfused in EDTA-coated tubes. PBMCs were isolated through centrifugation with Ficoll-Paque (GE Healthcare, Burnaby, BC, Canada). The PBMCs were than washed twice with HBSS (Life Technologies, Burlington, ON, Canada). T cells were isolated from the PBMCs by immune-magnetic isolation using CD3+ Dynabeads (Life Technologies). The beads were washed three times and incubated with the PBMCs for 45 min on a rotator at 4°C followed by a washing step (five times) with PBS/FBS. CD3+ T cells were then stored at −80°C until DNA extraction with the Wizard Genomic DNA Purification kit.

PFC dissection and DNA/RNA preparation from rats

After decapitation, brain tissues were dissected, immediately frozen on dry ice and stored at -80°C for later analyses. Dissections were performed according to the atlas of Paxinos and Watson [7]. In detail, the prefrontal cortex was dissected from 2-mm

thick slices (prefrontal cortex defined as Cg1, Cg3, and IL sub-regions corresponding to the plates 6–9). Isolation of DNA and RNA from the same rat specimen was performed using the AllPrep DNA/RNA Mini kit (Qiagen, Milan, Italy), in accordance with the instructions of the manufacturer.

Methylated DNA immunoprecipitation (MeDIP) analysis

MeDIP analyses have been performed as previously described in our studies [1,2]. Briefly, DNA was quantified by fluorometric analysis (Qubit® 2.0 Fluorometer, Life Technologies), 2 µg of DNA were sheared by sonication and methylated DNA was immunoprecipitated using 10µg of anti-5-methyl-cytosine (Cat. No. BI-MECY-0100, Eurogentec, Fremont, CA, USA). The human study comprised n = 10 infants with high levels of ELS and n = 8 infants with low levels of ELS. The monkey study involved 4 MR and 4 SPR 7-year-old male animals for PFC analysis and 5 MR and 5 SPR 2-year-old male animals for whole blood analysis. Buccal samples were analyzed from 3 MR and 3 SPR 2-year-old male animals. For CD3+ T cells analysis, pools of DNA were used, which consisted of: (i) 10 MR or 10 SPR monkeys sampled twice, i.e. at postnatal day 30, and (ii) 6 MR or 4 SPR monkeys sampled at age 2 years. Each DNA pool was subjected to 3 parallel MeDIP analyses (that is, 3 MR and 3 SPR pools per time point). For the rat study, samples of 4 Ctrl and 4 PNS male rats sacrificed at PND62 have been used for the hybridization on the microarray, while 4-7 males per group (Ctrl or PNS) were used for the MeDIP at PND7 and PND21. The DNA antibody complex was immunoprecipitated with protein G, and the methylated DNA was re-suspended in 0.25 ml of digestion buffer (50 mM TRisHCl pH = 8; 10 mM EDTA; 0.5 % SDS) and treated with 40 µg of proteinase K overnight at 55°C. The input and bound fractions were phenol/chloroform-extracted and ethanol-precipitated. Specificity for

methylated DNA and the absence of unspecific binding were validated through PCR analysis of an un-methylated (*β-actin* or *Gapdh*) and a methylated (*H19*) control gene (for primer sequences see supplementary Table 2). For MeDIP-chip, the input and bound fractions were amplified using the Whole Genome Amplification Kit (Sigma-Aldrich; St. Luis; MO; USA) and then labeled for microarray hybridization with Cy3-dUTP and Cy5-dUTP, respectively, using the CGH Enzymatic Labeling Kit (Agilent Technologies; Mississauga; ON; Canada) in accordance with the manufacturer´s instructions.

MeDIP microarray design, hybridization, scanning and analysis

For all microarray studies, custom promoter tiling microarray designs were used (Agilent Technologies). Probes were selected to tile all transcription start sites defined in the Ensembl database. Probes were placed approximately every 100 bp. For rat, approximately 400 K probes were selected to tile intervals covering -1 000 +200 bp around each transcription start site defined in the Ensembl database version 62 (Agilent design: 030107). Any genomic coordinates are given with respect to the rn4 (RGSC 3.4) rat genome assembly. For monkey PFC, the microarray design has already been described [2]. Approximately 240 K probes were selected to tile all transcription start sites defined in the Ensembl database version 46 (Agilent design: 018390). Any genomic coordinates are given with respect to the rheMac2 monkey genome assembly. For monkey whole blood, CD3+ and buccal cells, approximately 400K probes were selected to tile - 1 800 + 400 bp around each transcription start site defined in the Ensembl database version 64 (Agilent design: 0375811). Genomic coordinates are also given with respect to the rheMac2 genome assembly. For human CD34+ cells, the microarray design has already been described [1].

Approximately 400K probes were selected to tile – 2000 + 400 bp around each transcription start site defined in the Ensembl database version 59 (Agilent design: 024757). Genomic coordinates are given with respect to the hg19 (GRCh37) human genome assembly.

Probe intensities were extracted from scanned microarray images using Agilent's Feature Extraction 10.7.3.1 Image Analysis Software and analyzed using the R software environment for statistical computing (R Development Core Team, 2007) (http://www.r-project.org/). Log-ratios of the bound (Cy5) and input (Cy3) microarray channel intensities were computed for each microarray. Microarray quality was assessed using plots generated by the feature extraction software in addition to correlation matrix visualizations. Microarrays were normalized using quantile-normalization [8]. Estimates of DNA methylation levels based on microarray probe intensities were obtained using a Bayesian deconvolution algorithm [9]. Differential methylation between groups was determined in two stages. The first stage used linear models implemented in the 'limma' package [10] of Bioconductor [11] to compute a modified t-statistic at the individual probe level. As in typical microarray studies, the number of sample profiles is small so there is little information per probe from which to estimate probe variance. Hence, the modified t-statistic for each probe makes use of variance estimates derived from the other probes on the microarray. Correlation between technical replicates was modeled as a random effect using the "block" variable. An individual probe was called differentially methylated if the significance of its t-statistic was at most 0.05 (uncorrected for multiple testing) and the associated difference of log-normalized means between the groups was at least 0.5. In the second stage, differential

statistics per promoter were derived from the t-statistics of the probes within the promoter. In particular, the Wilcoxon rank-sum test was used to identify enrichment for probes within the promoter having large positive or large negative t-statistics. The resulting promoter p-values were adjusted for multiple testing by calculating false discovery rates using the Benjamini-Hochberg algorithm. A promoter was called differentially methylated if its false discovery rate was at most 0.2 and it contained at least one probe called differentially methylated, as defined above.

Validation using qPCR

Gene-specific quantitative real-time PCR validation of microarray (Q-MeDIP) was performed on the amplified-bound fraction for the same subjects used for microarray experiments. QPCR was performed in 1X Power SYBR Green Master Mix (Life technologies) using 4 - 10ng of DNA and 1.5 - 4 µM gene specific primers (supplementary Table 2) which were designed using Primer 3 (http://primer3.ut.ee/) free software. Relative enrichment of triplicate reactions was determined after normalizing from the input fraction in each sample using the $2^{(-\Delta\Delta Ct)}$ method. All data are expressed as group means ± SEM. To test for statistical significance the Student's *t* test was used (two-tailed), and the alpha level was set at 0.05.

QRT-PCR and analyses of mRNA levels in rats

Total RNA was quantified by spectrophotometric analysis (NanoDrop, Thermo Scientific) and samples were processed for real-time polymerase chain reaction (qPCR) to assess mRNA levels. An aliquot of each sample was treated with DNase to avoid DNA contamination.

RNA was analyzed by Taqman qRT-PCR instrument (CFX384 real time system, Bio-Rad Laboratories) using the iScriptTM one-step RT-PCR kit for probes (Bio-Rad

Laboratories). Samples were run in 384 well formats in triplicate as multiplexed reactions with a normalizing internal control (*36b4*). We choose *36b4* as internal standard for gene expression analyses since its expression was not affected by developmental changes and it was not altered by prenatal stress.

Probe and primer sequences of *36b4* (Forward Primer: TCAGTGCCTCACTCCATCAT; Reverse Primer: AGGAAGGCCTTGACCTTTTC; Taqman Probe: TGGATACAAAAGGGTCCTGG) and *Ankyrin-3* (Forward Primer: TCCTACAGAACGACACCAATG; Reverse Primer: CTCGGTTTAACAGCAACGTG; Taqman Probe: TGGCTTCACCCCACTCCACATAG) were purchased from Eurofins Genomics (Vimodrone, Italy).

Thermal cycling was initiated with an incubation at 50°C for 10 min (RNA retrotranscription) and then at 95°C for 5 min (TaqMan polymerase activation). After this initial step, 39 cycles of PCR were performed. Each PCR cycle consisted of heating the samples at 95°C for 10 s to enable the melting process and then for 30 s at 60°C for the annealing and extension reaction. Relative target gene expression was calculated according to the $2^{(-\Delta\Delta Ct)}$ method. Data are expressed as group means ± SEM. To test for statistical significance, a two-way ANalysis Of VAriance (ANOVA), followed by Fisher's LSD post-hoc comparisons was performed using SPSS for Mac OS X (Release 22.0.0.0), with 'PNS exposure' or 'AGE' as independent factors. A probability level of $p<0.05$ was taken as significant in every test.

Biochemical analyses in rats

Protein extraction, SDS-PAGE and western blot analysis

The prefrontal cortices of the second rat hemisphere were homogenized in a Teflon-glass potter in ice-cold 0.32 M sucrose buffer containing 1 mM HEPES, 1 mM $MgCl_2$, 1 mM $NaHCO_3$, and 0.1 mM phenylmethylsulfonyl fluoride, pH=7.4, in the presence of a complete set of protease (Roche) and phosphatase (Sigma-Aldrich) inhibitors. The homogenized tissue was centrifuged at 1 000g for 10 min to separate a pellet (P1) enriched in nuclear components from the supernatant (S1). S1 was then centrifuged at 13 000g for 15 min to obtain a clarified fraction of cytosolic proteins (S2). The pellet (P2), corresponding to the crude membrane fraction, was resuspended in 20 mM HEPES in the presence of a complete set of protease (Roche) and phosphatase (Sigma-Aldrich) inhibitors. An aliquot of the P2 was centrifuged at 100 000 g for 1 h. The pellet (P3) was resuspended in buffer containing 150 mM KCl, 0,5% Triton X-100 and 1mM HEPES in the presence of a complete set of protease (Roche) and phosphatase (Sigma-Aldrich) inhibitors with a Teflon-polycarbonate potter and centrifuged at 100 000 g for 1 h. The resulting supernatant (S4), referred as Triton X-100-soluble fraction (TSF), was stored at -20°C, while the pellet (P4), referred as the Triton X-100 insoluble fraction (TIF) which is enriched in the postsynaptic compartment, was homogenized in a glass-glass potter in 20 mM HEPES in the presence of a complete set of protease (Roche) and phosphatase (Sigma-Aldrich) inhibitors and stored at -20°C in the presence of glycerol 30%.

Total protein content was measured according to the Bradford Protein Assay procedure (Bio-Rad Laboratories), using bovine serum albumin as a calibration standard.

Qualitative enrichment analysis of ankyrin-G 190 kDa was performed on the above-mentioned subcellular fractions, while semi-quantitative protein analyses were

performed in the crude membrane fraction (P2). Equal amounts of total protein (5 µg for the TIF and 20 µg for all the other subcellular compartments) were run under reducing conditions (150 V at room temperature) on an SDS-polyacrylamide gel (7-8 % SDS-PAGE) and then electrophoretically transferred onto nitrocellulose membranes at 250 mA for 2 h at 4°C. Transfer efficiency was controlled by Ponceau S staining and pre-stained protein standards. Unspecific binding sites were blocked for 1 h in 10% non-fat dry milk in Tris-buffered saline solution containing 0.1% Tween-20 (TBS-T). Membranes were then incubated at 4°C over night with the following primary antibodies: rabbit polyclonal anti-ANKG primary antibody (Cat. No. sc-28561, Santa Cruz Biotechnology, 1:500 in 5 % non-fat dry milk in TBS-T), rabbit monoclonal anti-PSD95 primary antibody (Cat. No. 3450, Cell Signaling, 1:4 000 in 3 % non-fat dry milk in TBS-T), rabbit monoclonal anti-MECP2 primary antibody (Cat. No. 3456P, Cell Signaling, 1:1 000 in 5 % bovine serum albumin in TBS-T), rabbit monoclonal anti-synaptophysin primary antibody (Cat. No. D35E7, Cell Signaling, 1:1 000 in 3 % non-fat milk in TBS-T) and rabbit polyclonal anti-GLUR1 phosphoSer845 primary antibody (Cat. No. AB5849, Millipore, 1:500 in 5 % bovine serum albumin in TBS-T).

Membranes were then washed with TBS-T and incubated for 1 h at room temperature with a peroxidase-conjugated anti-rabbit IgG (Cat. No. BK4074S, Cell-Signaling Technology) (ANKG, 1:4 000 in 5 % non-fat milk in TBS-T; PSD95, 1:8 000 in 3 % non-fat milk in TBS-T; MECP2, 1:5 000 in 5 % non-fat milk in TBS-T; synaptophysin, 1:10 000 in 3 % non-fat milk in TBS-T; pGLUR1 S845, 1:2 000 in 3 % non-fat milk in TBS-T). Immunocomplexes were visualized by chemiluminescence using the ECL Western Blotting kit (Euroclone) according to the manufacturer's

instructions using the Chemidoc MP Imaging System (Bio-Rad Laboratories) and protein levels were calculated by measuring the optical density of the autoradiographic bands using Image-Lab software (Bio-Rad Laboratories). Results were standardized using β-Actin as control protein that was detected by evaluating the band density at 43 kDa after blocking the membranes with 10% non-fat dry milk and probing it with monoclonal mouse primary antibody anti-β-Actin (Cat. No. A5441, Sigma-Aldrich, 1:10 000 in 3 % non-fat dry milk in TBS-T), followed by the incubation with a peroxidase-conjugated antibody anti-mouse IgG (Cat. No. A4416, Sigma-Aldrich, 1:10 000 in 3 % non-fat dry milk in TBS-T dilution). To ensure that autoradiographic bands were in the linear range of intensity, different exposure times were used. Actin was employed as an internal standard because its expression is not regulated by the experimental paradigm used.

Data are expressed as group means ± SEM. To test for statistical significance the Student's *t* test was used (two-tailed), and the alpha level was set at 0.05.

Coimmunoprecipitation assay

Co-immunoprecipitation assays were performed as in Vastagh et al. [12] with the introduction of some methodological modifications. In detail, Aliquots of total cell homogenate (200 µg) were incubated in RIA buffer (400 mM NaCl, 20 mM EDTA, 20 mM Na_2HPO_4, 1% Nonidet P-40) and 0.1% sodium dodecylsulfate (SDS) with 3 µg of antibody against ankyrin-G (Cat. No. 75-146, Neuromab, clone N106/36) overnight at 4°C on a wheel, except for the 'white', in which the antibody was not added. Protein A/G agarose beads (Santa Cruz Biotechnology) were added and incubated for 2 h at 25°C on the wheel. Beads were collected by gravity and washed in RIA buffer containing 0.1 % SDS three times. Laemmli sample buffer was then added to the

samples and to the input (sample that did not undergo the IP and that were prepared with 10% of the starting material used for coimmunoprecipitation experiments, that is 20 µg of homogenate). The mixture was boiled for 10 minutes at 100°C. Beads were collected by gravity and the supernatant of the immunoprecipitated samples, of the input and of the white was loaded onto a 7% acrylamide/bisacrylamide gel for SDS–PAGE. The proteins were run at 30 mA and then electrophoretically transferred onto nitrocellulose membranes at 250 mA for 2 h at 4°C. We next performed Western blot analysis using mouse monoclonal anti-GLUR1 primary antibody (Cat. No. MAB-2263, Millipore, 1:1 000 in 3 % non-fat milk in TBS-T) and rabbit monoclonal anti-PSD95 primary antibody (Cell Signaling, 1:4 000 in 3 % non-fat dry milk in TBS-T). After, PSD95 was incubated for 1 h at room temperature with a peroxidase-conjugated anti-rabbit IgG (Sigma-Aldrich, 1:8 000 in 3 % non-fat milk in TBS-T), while GLUR1 was incubated with a peroxidase-conjugated antibody anti-mouse IgG (Sigma-Aldrich, 1:3 000 in 3 % non-fat dry milk in TBS-T). Results were standardized using ANKG as normalizing protein that was detected by evaluating the band density at 190 kDa after blocking the membranes with 10 % non-fat dry milk and probing it with rabbit polyclonal anti-ankyrin-G primary antibody (Santa Cruz Biotechnologies, 1:400 in 3 % non-fat milk in TBS-T), followed by the incubation with a peroxidase-conjugated antibody anti-rabbit IgG (Sigma-Aldrich, 1:3 000 in 5 % non-fat dry milk in TBS-T dilution). To ensure that autoradiographic bands were in the linear range of intensity, different exposure times were used.

Data are expressed as group means ± SEM. To test for statistical significance, the Student's *t* test was used (two-tailed), and the alpha level was set at 0.05.

Bioinformatics analysis

Venn diagrams

Venn diagrams (http://bioinformatics.psb.ugent.be/webtools/Venn/) were used to show all the possible overlaps between the datasets obtained from the different MeDIP-chip analyses performed in our different paradigms of adversities early in life.

Ingenuity Pathway Analysis

Ingenuity Pathway Analysis (IPA) bioinformatics resource (www. ingenuity.com) was used to analyze, integrate and interpret the lists of genes obtained from -omics experiments. IPA scores our dataset of interest against pathways in the Ingenuity Knowledge Base which houses a large database of biological and chemical relationships extracted from scientific literature, integrating data from a variety of experimental platforms. For each analysis, IPA ranks each function or pathway using the right tailed Fisher Exact Test, which measures the likelihood that the lists of genes are associated with a certain pathway/function.

Interaction between functional variation in *Ank3* and obstetric complications on working memory processing

Post-mortem investigation of Ank3 functional variation

Earlier results have indicated association of an intronic SNP in the *Ank3* gene, i.e. rs9804190, with gene expression levels in the superior temporal gyrus of patients with schizophrenia [13]. We therefore used the Braincloud dataset available at http://braincloud.jhmi.edu [14] to probe the association between rs9804190 and *Ank3* transcription levels in human *post mortem* prefrontal cortex (Brodmann Area 46). In particular, we investigated 268 brains of Caucasian (N=112), African American

(N=146), Asiatic (N=4) and Hispanic (N=6) non-psychiatric individuals (supplementary Table 3). Details of tissue acquisition, handling, processing, dissection, clinical characterization, neuropathological examinations, RNA extraction and quality control measures were described previously [14,15].

RNA from prefrontal grey matter was analyzed using spotted oligonucleotide microarrays yielding data from 30 176 gene expression probes and allowing us to focus on *Ank3* mRNA expression. In particular, total RNA was extracted, amplified and fluorescently labeled. Reference RNA was pooled from all samples and treated identically to sample RNAs. After normalization [16], log2 intensity ratios were further adjusted to reduce the impact of known and unknown sources of systematic noise on gene expression measures using surrogate variable analysis [14,17].

Data relative to 23 different transcription probes binding *Ank3* gene were available in the Braincloud dataset. We selected the hHA034365 probe based on its specific affinity for *Ank3* brain-specific isoform. In addition, differently from other available probes, the one on which we focused our analysis recognizes a central transcript region of the gene, thus softening possible artifacts due to low RNA integrity.

DNA from cerebellar tissue was investigated with Illumina Bead Chips producing 625,439 SNP genotypes called using the Bead Express software for each subject as previously described [14,17]. We focused our attention on rs9804190 genotype for association analysis. Thus, ANCOVA was performed, with rs9804190 genotype as the independent variable, *ANK3* mRNA expression as the dependent variable, and non-matched variables between groups (i.e. age, sex, RNA integrity number) and ethnicity as covariates of no interest. A statistical threshold of $p<0.05$ was used for this analysis.

In vivo fMRI and behavioral studies

Subjects

306 healthy Caucasian subjects from the region of Apulia, Italy, were enrolled in a behavioral study and were evaluated with the Structured Clinical Interview for DSM-IV [18] to exclude any psychiatric disorder. Further exclusion criteria were: history of drug or alcohol abuse, active drug use in the past year, head trauma with loss of consciousness, and any significant medical condition revealed by clinical assessment and magnetic resonance imaging. Handedness (Edinburgh Inventory) [19] and total IQ (WAIS-R) were also measured. All subjects participating to the protocol signed an informed consent before entering the study. The protocol was approved by the local ethics committee of the "Azienda Ospedaliero-Universitaria Consorziale Policlinico di Bari". 174 of these individuals (supplementary Table 4) also participated to a fMRI study. In both studies, all individuals performed the 1- and 2-back versions of the N-back task, eliciting two loads of working memory (WM) processing and were genotyped for rs9804190 (see below). Furthermore, mothers of all individuals completed the McNeil-Sjöström Scale [20], which allowed to split individuals based on the Obstetric Complications (OC) score (see below) [21]. Because of the small number of subjects carrying the TT genotype, these subjects and those carrying the GT genotype were collapsed in a single group (T carriers) in both the fMRI and the behavioral studies. Sample sizes were: a) in the fMRI sample, 57 CC with OC, 48 CC without OC, 38 T carriers with OC, 31 T carriers without OC; b) in the behavioral study sample, 115 CC with OC, 66 CC without OC, 86 T carriers with OC, 39 T carriers without OC. All groups were matched for socio-demographic variables (i.e. age, gender, total IQ, handedness, Hollingshead index) ($p > 0.05$).

N-Back task

Briefly, 'N-back' refers to how far back in the sequence of stimuli the subject had to recall. The stimuli consisted of numbers (1–4) shown in random sequence and displayed at the points of a diamond-shaped box. There was a visually paced motor task, which also served as a non-memory guided control condition (0-Back) that simply required subjects to identify the stimulus currently seen. In the working memory (WM) conditions, the task required recollection of a stimulus seen one (1-Back) or two stimuli (2-Back) previously while continuing to encode additionally incoming stimuli. Performance data were recorded as the percentage of correct responses (accuracy) and reaction time (ms).

During the fMRI data acquisition, subjects performed a blocked design version of the N-back task. In particular, there was a non memory-guided control condition (0-Back) that simply required subjects to identify the stimulus currently seen and the 1-Back and 2-Back conditions. The stimuli were arranged in eight blocks, each lasting 30 seconds: four blocks of the control condition alternating with four blocks of each WM condition. Stimuli were presented via a back-projection system. Responses were recorded through a fiber optic response box allowing measurement of percent accuracy and reaction time (in milliseconds). All subjects were trained on the task prior to the fMRI session.

Ank3 rs9804190 genotype determination

Genomic DNA of all individuals was isolated from whole blood using the QIAamp DNA Blood Maxi Kit (Qiagen, Venlo, Netherlands). Rs9804190 genotype determination was performed using 20 ng gDNA, which was amplified according to manufacturer's directions through a TaqMan® SNP Genotyping Probe (Assay ID

C_29667085_10) (Life Technologies, Carlsbad, CA, USA) in a MJ Mini Opticon thermal cycler (Bio-Rad, Hercules, CA, USA). Genotype calls were assessed with CFX Manager™ Software (Bio-Rad, Hercules, CA, USA). Minor allele homozygotes and heterozygous subjects were collapsed in one group in order to obtain sufficient sample sizes for the fMRI and behavioral analyses.

Obstetric complications (OC) collection and scoring

OC scores were determined through the McNeil-Sjöström Scale [20] that was administered to mothers of all participants. The purpose of the scale is to provide a standardized, functional system for the weighting of OC. Several hundred specific OC are included together with severity weights (representing an ordinal scale). The McNeil-Sjöström scale categorizes hundreds of different complications, rating each of them on a scale of 6 points, depending on its potential to determine a damage on the central nervous system of the newborn: 1) not harmful or relevant; 2) not likely harmful or relevant; 3) potentially but not clearly harmful or relevant; 4) potentially and clearly harmful or relevant; 5) potentially, clearly and greatly harmful/relevant; 6) very great harm to or deviation in offspring. Consistent with earlier studies [22] presence of OC were categorized depending on presence of at least one serious OC (severity score ≥3).

fMRI data acquisition

Blood oxygen level-dependent (BOLD) fMRI data were collected with a GE Signa 3T scanner (GE Healthcare), equipped with a standard quadrature head coil. A gradient-echo planar imaging sequence (repetition time, 2000 ms; echo time, 30 ms; thickness 4 mm; gap, 1 mm; flip angle, 90°; field of view, 24 cm; matrix, 64 x 64; 120

volumes for each run, 20 interleaved axial slices; duration: 4 min and 8 s) was used. The first four scans were discarded to allow for T1 equilibration effect.

fMRI data processing

Analysis of the fMRI data was completed using Statistical Parametric Mapping 8 (SPM8; http://www.fil.ion.ucl.ac.uk/spm). Images of each subject were slice timing corrected and pre-processed. In particular, standard procedures of realignment to the mean image were performed using the Realign and Unwarp algorithm provided in SPM8 in order to compensate for non-linear signal distortions potentially induced by head motion. Furthermore, movement parameters were extracted to eventually exclude subjects with excessive head motion (>2 mm translation, >2° rotation). Realigned images were resliced to a 2 mm isotropic voxel size, spatially normalized into a standard space (Montreal Neurological Institute template) with a 12 parameter affine model and smoothed using a 6 mm full-width half-maximum isotropic gaussian kernel to minimize noise and to account for residual inter-subject differences. A box car model convolved with the hemodynamic response function at each voxel was modeled. Linear contrasts were then computed producing a t statistical map for the 1 and 2 Back conditions, assuming the 0-Back condition as baseline.

Psychophysiological interaction (PPI) analysis

We next explored the interaction between *ANK3* and OC on prefronto-striatal connectivity. With this aim, psychophysiological interaction (PPI) analysis [23] was performed for each subject. In particular, we used a 5 mm ROI centered on the peak activity (x=-48, y=38, z=30) in left DLPFC as seed region. PPI was calculated using the first eigenvariate of individual raw activation time courses, extracted by using a

singular value decomposition method from a volume of interest centered on the subject-specific peak cluster within the seed region. These time courses were then mean centered, high-pass filtered and deconvolved. A general linear model was computed using three regressors: a physiological regressor (the time course response in the volume of interest), a psychological regressor (task design) and a PPI term, calculated as the cross-product of the previous two terms. Second-level random effects multiple regression were performed to investigate *Ank3* x OC interaction on prefrontal activity during performance of the 1- and 2-back WM tasks, using task load (1- and 2-back) as the repeated measures factor, and *Ank3* rs9804190 genotype as well as OC (absence/presence) as the between-subjects factor. We used a statistical threshold of $p<0.05$, family-wise error (FWE) small volume corrected for the left DLPFC, whose role is crucial in WM processing [24] and the greater involvement of the left portion of DLPFC during WM tasks eliciting both verbal and visuo-spatial processing [25,26].

Analysis of behavioral data

A repeated measure factorial ANOVA was performed, with genotype and OC presence/absence as the between-subjects factors, load (1- and 2-back) as the repeated-measures factor and behavioral accuracy (% of correct responses) or reaction time as the dependent variable. Tukey's test was used for post-hoc analyses.

References

1. Nieratschker V, Massart R, Gilles M, Luoni A, Suderman MJ, Krumm B *et al.* MORC1 exhibits cross-species differential methylation in association with early life stress as well as genome-wide association with MDD. *Transl Psychiatry* 2014; **4:e429.**
2. Provencal N, Suderman MJ, Guillemin C, Massart R, Ruggiero A, Wang D *et al.* The signature of maternal rearing in the methylome in rhesus macaque prefrontal cortex and T cells. *J Neurosci* 2012; **32**(44)**:** 15626-15642.
3. Massart R, Suderman M, Provencal N, Yi C, Bennett AJ, Suomi S *et al.* Hydroxymethylation and DNA methylation profiles in the prefrontal cortex of the non-human primate rhesus macaque and the impact of maternal deprivation on hydroxymethylation. *Neuroscience* 2014; **268:139-48.**
4. Nemoda Z, Massart R, Suderman M, Hallett M, Li T, Coote M *et al.* Maternal depression is associated with DNA methylation changes in cord blood T lymphocytes and adult hippocampi. *Transl Psychiatry* 2015; **5:e545.**
5. Luoni A, Berry A, Calabrese F, Capoccia S, Bellisario V, Gass P *et al.* Delayed BDNF alterations in the prefrontal cortex of rats exposed to prenatal stress: preventive effect of lurasidone treatment during adolescence. *Eur Neuropsychopharmacol* 2014; **24**(6)**:** 986-995.
6. Maccari S, Piazza PV, Kabbaj M, Barbazanges A, Simon H, Le Moal M. Adoption reverses the long-term impairment in glucocorticoid feedback induced by prenatal stress. *J Neurosci* 1995; **15**(1 Pt 1)**:** 110-116.
7. Paxinos G, Watson C. *The rat brain in stereotaxis coordinates*. Academic Press: New York1996.

8. Bolstad BM, Irizarry RA, Astrand M, Speed TP. A comparison of normalization methods for high density oligonucleotide array data based on variance and bias. *Bioinformatics* 2003; **19**(2)**:** 185-193.
9. Down TA, Rakyan VK, Turner DJ, Flicek P, Li H, Kulesha E *et al.* A Bayesian deconvolution strategy for immunoprecipitation-based DNA methylome analysis. *Nat Biotechnol* 2008; **26**(7)**:** 779-785.
10. Smyth GK, Michaud J, Scott HS. Use of within-array replicate spots for assessing differential expression in microarray experiments. *Bioinformatics* 2005; **21**(9)**:** 2067-2075.
11. Gentleman RC, Carey VJ, Bates DM, Bolstad B, Dettling M, Dudoit S *et al.* Bioconductor: open software development for computational biology and bioinformatics. *Genome Biol* 2004; **5**(10)**:** R80.
12. Vastagh C, Gardoni F, Bagetta V, Stanic J, Zianni E, Giampa C *et al.* N-methyl-D-aspartate (NMDA) receptor composition modulates dendritic spine morphology in striatal medium spiny neurons. *J Biol Chem* 2012; **287**(22)**:** 18103-18114.
13. Roussos P, Katsel P, Davis KL, Bitsios P, Giakoumaki SG, Jogia J *et al.* Molecular and genetic evidence for abnormalities in the nodes of Ranvier in schizophrenia. *Arch Gen Psychiatry* 2012; **69**(1)**:** 7-15.
14. Colantuoni C, Lipska BK, Ye T, Hyde TM, Tao R, Leek JT *et al.* Temporal dynamics and genetic control of transcription in the human prefrontal cortex. *Nature* 2011; **478**(7370)**:** 519-523.
15. Lipska BK, Deep-Soboslay A, Weickert CS, Hyde TM, Martin CE, Herman MM *et al.* Critical factors in gene expression in postmortem human brain: Focus on studies in schizophrenia. *Biological psychiatry* 2006; **60**(6)**:** 650-658.

16. Colantuoni C, Henry G, Zeger S, Pevsner J. SNOMAD (Standardization and NOrmalization of MicroArray Data): web-accessible gene expression data analysis. *Bioinformatics* 2002; **18**(11)**:** 1540-1541.
17. Leek JT, Storey JD. Capturing heterogeneity in gene expression studies by surrogate variable analysis. *PLoS genetics* 2007; **3**(9)**:** 1724-1735.
18. Williams JB, Gibbon M, First MB, Spitzer RL, Davies M, Borus J *et al.* The Structured Clinical Interview for DSM-III-R (SCID). II. Multisite test-retest reliability. *Arch Gen Psychiatry* 1992; **49**(8)**:** 630-636.
19. Oldfield RC. The assessment and analysis of handedness: the Edinburgh inventory. *Neuropsychologia* 1971; **9**(1)**:** 97-113.
20. McNeil TF, Cantor-Graae E, Sjostrom K. Obstetric complications as antecedents of schizophrenia: empirical effects of using different obstetric complication scales. *J Psychiatr Res* 1994; **28**(6)**:** 519-530.
21. Verdoux H, Sutter AL. Perinatal risk factors for schizophrenia: diagnostic specificity and relationships with maternal psychopathology. *Am J Med Genet* 2002; **114**(8)**:** 898-905.
22. Verdoux H, Sutter AL, Glatigny-Dallay E, Minisini A. Obstetrical complications and the development of postpartum depressive symptoms: a prospective survey of the MATQUID cohort. *Acta Psychiatr Scand* 2002; **106**(3)**:** 212-219.
23. Friston KJ, Buechel C, Fink GR, Morris J, Rolls E, Dolan RJ. Psychophysiological and modulatory interactions in neuroimaging. *Neuroimage* 1997; **6**(3)**:** 218-229.
24. Callicott JH, Mattay VS, Bertolino A, Finn K, Coppola R, Frank JA *et al.* Physiological characteristics of capacity constraints in working memory as revealed by functional MRI. *Cereb Cortex* 1999; **9**(1)**:** 20-26.

25. Rottschy C, Langner R, Dogan I, Reetz K, Laird AR, Schulz JB *et al.* Modelling neural correlates of working memory: a coordinate-based meta-analysis. *Neuroimage* 2012; **60**(1)**:** 830-846.
26. Wager TD, Smith EE. Neuroimaging studies of working memory: a meta-analysis. *Cogn Affect Behav Neurosci* 2003; **3**(4)**:** 255-274.

Supplementary Table 1
Phenotypic characteristics of mothers and infants

Supplementary Table 1a: Summary of the phenotypic assessment of mothers and infants at two time points early in life

	Prenatal / 3rd Trimester	**Perinatal / birth**
Exposure to early life stress (ELS)	Perceived stress (PSS[1]) Prenatal distress (PDQ[2]) Life events (LES[3]) Social support (Soz-U.[4]) Socio-demographic data Maternal health risk behavior (e.g. smoking) Psychosocial risks	Pre- and perinatal complications Perinatal stressors (e.g. asphyxia, caesarian, preterm birth) Pregnancy & obstetric history (birth weight, gestational age, birth complications)
Maternal mental & physical health	Maternity log data semi- standardized neuropsychiatric diagnostic interview (M.I.N.I.[5]) Depression screening (EPDS[6]) Anxiety screening (STAI-S[7], STAI-T[7], ASQ[8]) Anthropometry Individual & family history of metabolic and other medical disorders	

1, perceived stress scale; 2, prenatal distress questionnaire; 3, life experiences survey; 4, social support questionnaire; 5, Mini-international neuropsychiatric interview; 6, Edinburgh postnatal depression scale; 7, state- trait anxiety inventory; 8, anxiety screening questionnaire

Supplementary Table 1

Phenotypic characteristics of mothers and infants

Supplementary Table 1b: Summary of the information about psychopathology, socioeconomic-, psychosocial- and perceived stress of the extreme group of mothers expressed as mean ± SD1 or percentage

Variable	High prenatal ELS (n =10)	Low prenatal ELS (n =8)	*p* value
Maternal psychopathology			
EPDS Score[3]	15.40 ± 4.95	2.13 ± 1.25	0
STAI-S Score[3]	52.60 ± 13.32	32.62 ± 4.81	0.001
STAI-T Score[3]	50.90 ± 10.50	28.75 ± 4.53	0
ASQ Score[3]	5.40 ± 1.84	0.25 ± 0.46	0
M.I.N.I. Diagnosis[4]			
none	20%	100%	0
depressive disorders	50%	0%	0.015
anxiety disorder	10%	0%	ns[2]
Current psychiatric disorder[4] (%)			
none	30%	100%	0.001
depressive disorder	50%	0%	0.015
anxiety disorder	10%	0%	ns[2]
Perceived stress			
PSS Score[3]	32.70 ± 6.93	15.25 ± 3.92	0
PDQ Score[3]	23.70 ± 8.06	8.63 ± 4.37	0
Socioeconomic and psychosocial stress			
LES-negative events Score[3]	8.50 ± 6.98	1.63 ± 1.06	0.013
Soz-U Score[3]	37.80 ± 10.68	48.00 ± 6.78	0.026
Living without a partner[4] (%)	40%	0%	0.037
Encouragement (Partner)[4] (%)	70%	100%	ns[2]
Separation(s) in the last year[4]	50%	0%	0.015
Daily arguments[4]	20%	0%	ns[2]
Physical conflicts within the preceding 12 months[4]	60%	0%	0.005
Composition of household >one person /room[4]	30%	0%	0.037
No graduation[4] (%)	20%	0%	ns[2]
No professional education[4] (%)	40%	0%	0.037
Monthly income per household ≤ 1750 Euro[4] (%)	70%	0%	0.001
Financial debt[4] (%)	50%	0%	0.015

1, standard deviation; 2, not significant; 3, the first eight main variables of the principal component analysis (PCA);
4, the twelve prenatal stressors which generate the adversity score as the ninth main variable of the PCA

Supplementary Table 1
Phenotypic characteristics of mothers and infants

Supplementary Table 1c: Summary of the demographic characteristics and general medical status of mothers and infants included in the methylome analysis expressed as mean ± SD or percentage

Variable	High prenatal ELS (n = 10)	Low prenatal ELS (n = 8)	*p* value
Maternal Age (in years)	24.10 ± 5.43	34.00 ± 3.30	0.000
Smoking during early pregnancy (4^{th} to 12^{th} wpma[1]; %)	70%	12.50%	0.013
Cigarettes in total (4^{th} to 12^{th} wpma[1]) **Range of cigarettes smoked**	297.70 ± 412.68 0-1092	3.00 ± 8.50 0-24	0.050
Smoking during late pregnancy (3^{rd} trimester, %)	40%	0%	0.037
Cigarettes per day (3^{rd} trimester) **Range of cigarettes smoked**	3.30 ± 6.31 0-17	0 0	ns[4]
Alcohol intake during early pregnancy (4^{th} to 12^{th} wpma[1]; %)	30%	75%	ns[4]
Total alcohol intake (4^{th} to 12^{th} wpma[1] in g[5])	75.50 ± 187.18	23.50 ± 22.62	ns[4]
Alcohol during late pregnancy (3^{rd} trimester; %)	0%	0%	ns[4]
Primiparous	30%	37.50%	ns[4]
Number of risk factors in the maternity log	4.60 ± 2.38	3.17 ± 1.51	ns[4]
Pre-Pregnancy BMI[2]	25.53 ± 7.08	21.69 ± 4.57	ns[4]
Gestational diabetes (%)	20%	0%	ns[4]
Gestational age at birth (wpma[1])	38.70 ± 2.00	39.63 ± 1.60	ns[4]
Infant's Gender (%), male	50%	37.50%	ns[4]

1, weeks postmenstrual age; 2, body mass index; 3, standard deviation; 4, not significant; 5, gram

Supplementary Table 2

Sequences of primers used for enrichment analyses of methylated DNA and for quantitative PCR (QPCR) validation of MeDIP data.

Human		
Gene	Forward	Reverse
H19	5´- GAGCCGCACCAGATCTTCAG-3´	5´-TTGGTGGAACACACTGTGATCA-3´
ß-actin	5´- CCAACGCCAAAACTCTCCC-3´	5´- AGCCATAAAAGGCAACTTTCG-3´
Monkey		
Gene	Forward	Reverse
H19	5′-TTGGTGGAACACGCTGTGATCA-3′	5′-GAGCCGCACCAGGTCTTCAG-3′
Gapdh	5′-TTTCTTTCCTTTCGCGCTCTG-3′	5′-CCATTCATTTCCTTCCCGGTT-3′
Rat		
Gene	Forward	Reverse
H19	5´- CCAAGACAGAAGGGGACCAT-3´	5´- TAGATTTGGGGTTCGCCTGT-3´
ß-actin	5´- TGGGATAGTGTCCACAAGGG -3´	5´- GAAGAGTTTGGCGATGGGTG -3´
Ankyrin-3	5′- CAGGGGCTGTATTCTAGCAACT-3′	5′- CCCCTCCGTCTCACACTATTTT-3′

H19 = methylated control; *ß-actin, Gapdh* = un-methylated control

Supplementary Table 3

Characteristics of the Braincloud sample.

Sample Size	Female (Male)	Age	RIN	PMI	pH
268	92 (176)	27.9 ± 22.2	8.4 ± 0.9	26.4 ± 17.1	6.5 ± 0.3

All the data are expressed as mean ± SD

Supplementary Table 4

Characteristics of the samples used for the human behavioral and fMRI WM studies.

	Behavior	fMRI
N	306	174
Gender (M/F)	138/168	81/93
Age	26.0±6.2	26.9±6.4
Handedness	0.7±0.4	0.7±0.5
Parental socioeconomic status	39.9±16.5	40.9±16.4
IQ	107.4±11.6	109.8±11.8

Supplementary Table 5

Top diseases and biological functions associated with differentially methylated genes in the rat prefrontal cortex at PND62 after prenatal exposure to stress.

Diseases and Disorders	***p* value**
Neurological Disease	4.22E-09
Organismal Injury and Abnormalities	3.46E-08
Cardiovascular Disease	2.67E-07
Hereditary Disorder	4.71E-07
Psychological Disorders	4.71E-07
Molecular and Cellular Functions	***p* value**
Molecular Transport	2.56E-08
Cell Cycle	8.28E-08
Cell-To-Cell Signaling and Interaction	4.30E-07
Cellular Development	2.82E-06
Cellular Growth and Proliferation	5.01E-06
Physiological System Development and Function	***p* value**
Nervous System Development and Function	2.56E-10
Organ Morphology	1.72E-05
Embryonic Development	2.40E-05
Organ Development	2.40E-05
Organismal Development	2.40E-05

Supplementary Table 6

List of probes showing differential methylation in the eight genes resulting from the overlap of different paradigms of early life stress exposure in different species and tissues.

Gene name	Higher methylation in	Rat PFC (postnatal day 62)		Monkey PFC (7 years old)		Monkey CD3+ (day 30 old)		Monkey CD3+ (2 years old)		Human CD34+ (cord blood)	
		diff meth probe	*q* value	diff meth probe	*q* value	diff meth probe	*q* value	diff meth probe	*q* value	diff meth probe	*q* value
Ank3	Stress	chr20:19580638-19580697	0.141959	chr9:76713019-76713067	0.143384	chr9:76897059-76897118	0.015381	chr9:76897219-76897278	0.100842	chr10:61900618-61900677	0.060659
				chr9:76713128-76713178	0.143384	chr9:76897099-76897158	0.015381	chr9:76897299-76897358	0.100842	chr10:61901941-61902000	0.185321
				chr9:76713244-76713294	0.143384	chr9:76897139-76897198	0.015381	chr9:76899099-76899158	0.017648		
				chr9:76713473-76713532	0.143384	chr9:76897179-76897238	0.015381	chr9:76899139-76899198	0.017648		
						chr9:76897299-76897358	0.015381				
						chr9:76897379-76897438	0.032022				
						chr9:77144454-77144513	0.015059				
						chr9:77144854-77144913	0.015059				
						chr9:77144934-77144993	0.015059				
	Control	chr20:19420344-19420403	0.114085	✗		✗		✗		chr10:62149544-62149598	0.146104
		chr20:19420705-19420764	0.114085							chr10:62149595-62149639	0.146104
Cnga4	Stress	chr1:163137594-163137649	0.000065	chr14:65936603-65936662	0.086013	✗		✗		chr11:6256207-6256251	0.022758
		chr1:163137327-163137372	0.000065	chr14:65936702-65936758	0.086013					chr11:6256284-6256328	0.022758
				chr14:65936991-65937039	0.086013						
				chr14:65968017-65968072	0.191803						
				chr14:65968116-65968172	0.191803						
	Control	✗		✗		chr14:65967196-65967255	0.000299	chr14:65967116-65967175	0.018034	chr11:6260165-6260210	0.095651
						chr14:65967276-65967335	0.000299	chr14:65967316-65967375	0.018034	chr11:6260273-6260320	0.095651
						chr14:65967476-65967535	0.000054	chr14:65967396-65967455	0.018034	chr11:6260342-6260386	0.095651
						chr14:65967516-65967575	0.000054	chr14:65967476-65967535	0.018034		
						chr14:65967556-65967615	0.000054	chr14:65967516-65967575	0.018034		
						chr14:65967596-65967655	0.000054				
						chr14:65967676-65967735	0.000054				
						chr14:65967716-65967775	0.000054				
						chr14:65967916-65967975	0.000054				
						chr14:65967956-65968015	0.000054				
						chr14:65968036-65968095	0.000054				
						chr14:65968076-65968135	0.000054				
Dars2	Stress	chr13:76629115-76629165	0.005713	✗		chr1:203489067-203489126	0.009011	✗		✗	
						chr1:203489147-203489206	0.009011				
						chr1:203489227-203489286	0.009011				
						chr1:203489307-203489366	0.009011				
	Control	✗		chr1:203460771-203460815	0.135128	chr1:203460535-203460594	0.016604	chr1:203460415-203460474	0.041125	chr1:173793860-173793907	0.152082
				chr1:203460900-203460956	0.135128	chr1:203460615-203460674	0.016604	chr1:203461095-203461154	0.041125		
				chr1:203460981-203461036	0.135128						
Gabrg2	Stress	chr10:27127411-27127470	0.186921	chr6:158458645-158458691	0.143637	chr6:158458012-158458071	0.056063	chr6:158457932-158457991	0.161943	chr5:161493755-161493814	0.034243
						chr6:158458052-158458111	0.056063	chr6:158458892-158458951	0.084601	chr5:161494278-161494337	0.034243
						chr6:158458412-158458471	0.001017				
						chr6:158458772-158458831	0.001017				
						chr6:158458852-158458911	0.001017				
						chr6:158458892-158458951	0.001017				
	Control	chr10:27130458-27130517	0.140810	✗		✗		✗		✗	
		chr10:27130465-27130524	0.140810								
		chr10:27130768-27130827	0.140810								
		chr10:27130966-27131025	0.140810								
		chr10:27131178-27131237	0.140810								
		chr10:27131397-27131456	0.140810								
		chr10:27104323-27104382	0.058220								
		chr10:27104987-27105046	0.164937								
Htr4	Stress	✗		✗		✗		chr6:145085774-145085833	0.132238	chr5:148034080-148034124	0.010424
								chr6:145085814-145085873	0.132238	chr5:148034081-148034125	0.010424
								chr6:145085894-145085953	0.132238	chr5:148034081-148034125	0.010424
								chr6:145163181-145163240	0.124103	chr5:148034443-148034495	0.010424
								chr6:145163261-145163320	0.124103		
	Control	chr18:58416260-58416319	0.164027	chr6:145163771-145163827	0.149301	chr6:145163981-145164040	0.100424	✗		✗	
Lphn2	Stress	✗		chr1:84116661-84116711	0.130892	chr1:84117017-84117076	0.077143	chr1:84506033-84506092	0.184338	chr1:81771325-81771384	0.176615
						chr1:84117257-84117316	0.077143	chr1:84506193-84506252	0.184338		
						chr1:84117337-84117396	0.077143	chr1:84742988-84743047	0.042337		
						chr1:84117617-84117676	0.077143	chr1:84743548-84743607	0.042337		
						chr1:84505713-84505772	0.179901				
						chr1:84505993-84506052	0.179901				
						chr1:84506033-84506092	0.179901				
						chr1:84506193-84506252	0.179901				
	Control	chr2:247201889-247201948	0.067236	✗		✗		✗		✗	
		chr2:247268119-247268163	0.012587								
Slc22a2	Stress	✗		✗		✗		chr4:157239558-157239617	0.005790	chr6:160699502-160699557	0.195967
								chr4:157240038-157240097	0.005790		
								chr4:157240078-157240137	0.005790		
	Control	chr1:42443429-42443481	0.008736	chr4:157247817-157247861	0.198596	chr4:157238718-157238777	0.024379	✗		✗	
				chr4:157248155-157248199	0.198596						
Tiam1	Stress	chr11:30218874-30218928	0.027820	✗		chr3:15243884-15243943	0.015329	✗		✗	
		chr11:30218705-30218752	0.027820			chr3:15243964-15244023	0.015329				
		chr11:30218643-30218689	0.027820								
	Control	✗		chr3:14951518-14951562	0.123568	chr3:15241884-15241943	0.064748	chr3:15242844-15242903	0.037906	chr21:32932342-32932386	0.146465
						chr3:15242084-15242143	0.064748			chr21:32932167-32932211	0.146465
						chr3:15242164-15242223	0.003634				
						chr3:15242524-15242583	0.003634				
						chr3:15242564-15242623	0.003634				
						chr3:15242644-15242703	0.003634				
						chr3:15242684-15242743	0.003634				
						chr3:15242724-15242783	0.003634				
						chr3:15242764-15242823	0.003634				

In the conditions marked with ✗, we found no probes differentially methylated between the control and stressed groups.

Supplementary Table 7

Summary of the probes associated with Ank3 and Gabrg2 which are differentially methylated between control and stressed groups.

	Higher methylation in	Rat PFC	Monkey PFC (7 years old)	Monkey CD3+ (day 30 old)	Monkey CD3+ (2 years old)	Human CD34+ (cord blood)	Monkey Whole Blood (2 years old) diff meth probe	*q* value	Monkey Buccal Cells (2 years old) diff meth probe	*q* value
Ank3	Stress	✓	✓	✓	✓	✓	chr9:77074944-77075003	0.038705	chr9:76897139-76897198	0.158048
							chr9:77074984-77075043	0.038705		
	Control	✓	✗	✗	✗	✓	✗		✗	
Gabrg2	Stress	✓	✓	✓	✓	✓	✗		✗	
	Control	✓	✗	✗	✗	✗	chr6:158457292-158457351	0.001338	chr6:158457612-158457671	0.044732
							chr6:158457372-158457431	0.001338	chr6:158457772-158457831	0.094282
							chr6:158457852-158457911	0.001338	chr6:158458332-158458391	0.102620
							chr6:158458092-158458151	0.001338	chr6:158458372-158458431	0.102620
							chr6:158458132-158458191	0.001338		

In the conditions marked with ✗, we found no probes differentially methylated between the control and stressed groups, while in the conditions marked with ✓ we found probes differentially methylated between the control and stressed groups.

Supplementary Table 8

List of the p values and effect size estimates ('differential') associated with probes, mapping Ank3, which were more methylated in the stressed group compared to the controls.

Samples	diff meth probe	*p* value	differential (log2)
Rat PFC (postnatal day 62)	chr20:19580638-19580697	0.049	0.913
Monkey PFC (7 years old)	chr9:76713019-76713067	0.014	1.360
	chr9:76713128-76713178	0.011	1.160
	chr9:76713244-76713294	0.037	1.090
	chr9:76713473-76713532	0.024	1.590
Monkey CD3+ (day 30 old)	chr9:76897059-76897118	0.010	0.966
	chr9:76897099-76897158	0.017	1.038
	chr9:76897139-76897198	0.009	1.072
	chr9:76897179-76897238	0.043	0.827
	chr9:76897299-76897358	0.024	0.871
	chr9:76897379-76897438	0.034	0.768
	chr9:77144454-77144513	0.012	0.926
	chr9:77144854-77144913	0.039	1.085
	chr9:77144934-77144993	0.022	0.948
Monkey CD3+ (2 years old)	chr9:76897219-76897278	0.040	0.551
	chr9:76897299-76897358	0.022	0.846
	chr9:76899099-76899158	0.047	0.562
	chr9:76899139-76899198	0.046	0.615
Human CD34+ (cord blood)	chr10:61900618-61900677	0.007	0.519
	chr10:61901941-61902000	0.026	0.894
Monkey Whole Blood (2 years old)	chr9:77074944-77075003	0.027	0.552
	chr9:77074984-77075043	0.038	1.482
Monkey Buccal Cells (2 years old)	chr9:76897139-76897198	0.007	1.651